scientific reports

Check for updates

OPEN

A novel artificial intelligence based multistage controller for load frequency control in power systems

Mostafa Jabari[1], Davut Izci[2,3], Serdar Ekinci[2], Mohit Bajaj[4,5,6]✉, Vojtech Blazek[7] & Lukas Prokop[7]

The imbalance between generated power and load demand often causes unwanted fluctuations in the frequency and tie-line power changes within a power system. To address this issue, a control process known as load frequency control (LFC) is essential. This study aims to optimize the parameters of the LFC controller for a two-area power system that includes a reheat thermal generator and a photovoltaic (PV) power plant. An innovative multi-stage TDn(1 + PI) controller is introduced to reduce the oscillations in frequency and tie-line power changes. This controller combines a tilt-derivative with an N filter (TDn) with a proportional-integral (PI) controller, which improves the system's response by correcting both steady-state errors and the rate of change. This design enhances the stability and speed of dynamic control systems. A new meta-heuristic optimization technique called bio-dynamic grasshopper optimization algorithm (BDGOA) is used for the first time to fine-tune the parameters of the proposed controller and improve its performance. The effectiveness of the controller is evaluated under various load demands, parameter variations, and nonlinearities. Comparisons with other controllers and optimization algorithms show that the BDGOA-TDn(1 + PI) controller significantly reduces overshoot in system frequency and tie-line power changes and achieves faster settling times for these oscillations. Simulation results demonstrate that the BDGOA-TDn(1 + PI) controller significantly outperforms conventional controllers, achieving a reduction in overshoot by 75%, faster settling times by 60%, and a lower integral of time-weighted absolute error by 50% under diverse operating conditions, including parameter variations and nonlinearities such as time delays and governor deadband effects.

Keywords Artificial intelligence, Intelligent control, Bio-dynamic grasshopper optimization algorithm, Load frequency control, Hybrid power systems, Multi-stage controller, Advanced optimization methods

Nomenclature

LFC	Load frequency control
PV	Photovoltaic
PI	Proportional-integral
TD*n*	Tilt-derivative with an N filter
BDGOA	Bio-dynamic grasshopper optimization ALGORİTHM
RESs	Renewable energy sources
PID	Proportional integral derivative
GA	Genetic algorithm
FA	Firefly algorithm
SSA	Salp swarm algorithm
MWOA	Modified whale optimization algorithm
GTO	Gorilla troops optimization
MPPT	Maximum power point tracking
WOA	Whale optimization algorithm

[1]Faculty of Electrical Engineering, Sahand University of Technology, Tabriz, Iran. [2]Department of Computer Engineering, Batman University, Batman, Turkey. [3]Applied Science Research Center, Applied Science Private University, Amman 11931, Jordan. [4]Department of Electrical Engineering, Graphic Era (Deemed to be University), Dehradun 248002, India. [5]College of Engineering, University of Business and Technology, Jeddah 21448, Saudi Arabia. [6]Graphic Era Hill University, Dehradun 248002, India. [7]ENET Centre, VSB—Technical University of Ostrava, Ostrava 708 00, Czech Republic. ✉email: thebestbajaj@gmail.com

CES	Capacitive energy storage
DRP	Demand response program
PIDn	Proportional integral derivative with derivative filter
FOPI	Fractional order proportional integral
BOA	Bonobo optimization algorithm
WOA	Whale optimization algorithm
AGC	Automatic generation control
FOPID	Fractional order proportional integral derivative
FLiPID	Hybrid fuzzy logic intelligent PID
PSO	Particle swarm optimization
BD	Boiler dynamic
MSCA	Modified sine cosine algorithm
PDO	Prairie dog optimization
ICA	Imperialist competition algorithm
PSO-TVAC	Particle swarm optimization with time varying acceleration coefficients
TD	Time delay
GDB	Governor deadband
BWOA	Black widow optimization algorithm
SFLA	shuffled frog-leaping algorithm
$\boldsymbol{\tau_G}$	Governor time constant
$\boldsymbol{\tau_T}$	Turbine time constant
$\boldsymbol{\tau_R}$	Reheater time constant
$\boldsymbol{\tau_{PS}}$	Power system time constant
$\boldsymbol{K_G}$	Governor gain
$\boldsymbol{K_T}$	Turbine gain
$\boldsymbol{K_R}$	Reheater gain
$\boldsymbol{K_{PS}}$	Power system gain
ACE	Area control error
$\boldsymbol{\Delta f_1}$	Area-1 frequency changes
$\boldsymbol{\Delta f_2}$	Area-2 frequency changes
$\boldsymbol{\Delta P_{tie}}$	Tie-line power connecting the two regions
R	Regulation droop
B	Frequency bias parameter
PC	Pressure control
FS	Fuel system
BS	Boiler storage
K_D, K_P, K_I	Derivative, proportional, integral gains of controller
OS	Overshoot
Tp	Peak time
N	Controller filter
n	Controller filter
GOA	Grasshopper optimization algorithm
e_p	Elimination phase
e_t	Elimination percent
T_h	Threshold
$\boldsymbol{\omega}$	Inertial coefficient
OF	Objective function
GEO	Golden eagle optimization
POA	Pelican optimization algorithm
λ, μ	Integral and derivative order
IAE	Integral of absolute error
ITAE	Integral of time weighted absolute error
ISE	Integral of square error
ITSE	Integral of time weighted square error
K_1, K_2, K_3	Boiler dynamic system parameters
ST	Settling time
US	Undershoot
C_B	Boiler storage time constant
T_d	Fuel ignition system delay time
T_F	Fuel system time constant
K_{IB}	Boiler integrator gain
T_{IB}	Proportional integral ratio of the gains
T_{RB}	Lead–lag compensator time constant
T(s)	Controller output signal
T_1(s)	Multi stage controller's initial stage control signal

The increasing integration of renewable energy sources (RESs), such as photovoltaic (PV) systems, into traditional power grids has brought new challenges to load frequency control (LFC)[1–3]. The combination of fluctuating renewable energy generation with the inherent dynamics of thermal power plants creates instability in power

system frequency[4] and tie-line power, leading to potential operational inefficiencies[5]. This study is motivated by the need to design an advanced control mechanism that can effectively manage the dynamic interactions between renewable and conventional energy sources while maintaining frequency stability and minimizing power fluctuations. By improving the efficiency and reliability of hybrid power systems, the research aims to address critical issues related to the stability and performance of modern power grids.

Related works

The control and optimization of hybrid power systems, particularly in the context of load frequency control (LFC), have garnered significant attention due to the increasing integration of renewable energy sources and the complexities of managing hybrid systems. Dunna et al.[6] proposed a super-twisting MPPT control for grid-connected PV/battery systems using higher-order sliding mode observers, emphasizing the enhancement of stability under fluctuating renewable energy conditions. However, their focus on grid stability does not extend to addressing the intricate frequency regulation challenges posed by hybrid systems incorporating thermal power plants. Similarly, Izci et al.[7] developed a fractional-order PID plus double-derivative controller for automatic voltage regulation using the mountain gazelle optimizer. While this study demonstrates the potential of advanced fractional-order controllers in improving system stability, it primarily targets voltage regulation, leaving the domain of frequency control in hybrid systems unexplored.

Expanding on controller tuning methodologies, Aribowo et al.[8,9] employed gradient-based and modified mountain gazelle optimizers for PID controller tuning in DC motor systems. These studies highlight the critical role of optimization algorithms in enhancing controller performance. While focused on DC motor applications, such optimization approaches resonate with the use of bio-dynamic grasshopper optimization algorithm (BDGOA) in fine-tuning LFC parameters for hybrid power systems. Premkumar et al.[10] further explored hybrid power systems by employing a multi-objective optimization approach for stochastic renewable energy sources and FACTS devices, demonstrating the need for sophisticated control strategies to manage system uncertainties. This study contributes to understanding system complexities, yet it focuses on operational optimization rather than specific challenges related to frequency stability and oscillation reduction, as addressed in this research.

Pandya et al.[11] introduced a RIME algorithm-based approach for techno-economic analysis in hybrid power systems, accounting for uncertainties in security-constrained load dispatch. This work underscores the significance of managing uncertainties, a challenge also addressed in this study through the robust design of the BDGOA-tuned TDn(1 + PI) controller. Alsmadi et al.[12] extended this discussion by integrating fuzzy logic with model order reduction for digital systems, emphasizing the adaptability of intelligent control techniques. While fuzzy logic control enhances system flexibility, the integration of tilt-derivative control with proportional-integral action in the present study achieves superior performance under nonlinear and uncertain conditions.

In the realm of dynamic systems, Abualigah et al.[13] and Alrashed et al.[14] explored optimized PID controller designs for aircraft pitch control and dynamic voltage restorers, respectively, leveraging novel optimization techniques like the Sinh-Cosh Optimizer and IGWO algorithm. These studies demonstrate the applicability of advanced optimization in diverse fields but lack the focus on hybrid energy systems. Similarly, Fadheel et al.[15] proposed a hybrid sparrow search optimization-based fractional virtual inertia control for frequency regulation in microgrids, showcasing the potential of hybrid optimization techniques. While their approach targets microgrid applications, this research addresses the broader challenge of multi-area power systems, enhancing both inter-area frequency stability and tie-line power regulation.

The contributions of Abualigah et al.[16–18] in refining optimization algorithms, such as the artificial rabbits optimizer and modified artificial hummingbird algorithm, align with the growing trend of employing bio-inspired optimization techniques. These studies focus on improving system stability and efficiency across applications like automatic voltage regulation and cruise control systems. The integration of BDGOA with a multi-stage controller in this study achieves significant reductions in overshoot and settling times in hybrid power systems, representing a distinct advancement. Altawil et al.[19] explored the slap swarm algorithm for fractional-order PI controller optimization in grid-connected PV systems, emphasizing the importance of controller adaptability. The current study advances this notion by addressing both transient and steady-state performance in hybrid systems with varying operational conditions.

Finally, Sarayrah et al.[20] investigated predictive damping control strategies for inter-area power systems, focusing on improving dynamic stability. Their approach highlights the importance of predictive strategies in modern power grids, a principle mirrored in this study through the use of a multi-stage controller design that anticipates and mitigates frequency fluctuations. Additionally, Sarayrah et al.[21] examined a damping control strategy employing predictive modeling for inter-area oscillations in power systems. Their work emphasizes predictive and proactive control mechanisms for enhancing system stability. However, while focused on inter-area oscillations, the study does not delve into hybrid systems with renewable energy sources, where the dynamics of PV and thermal generators significantly complicate control requirements.

Various controllers have been proposed in recent years to enhance the performance of LFC systems[3,22]. Among these, proportional integral (PI)[23] and proportional integral derivative (PID)[24] controllers are widely used due to their simplicity and ease of implementation. However, conventional PI and PID controllers often fall short in addressing the nonlinearities and complexities of hybrid power systems[25,26]. To overcome these limitations, more multi-stage controllers have been developed[27–29]. These controllers not only address steady-state errors but also improve the dynamic response by managing the rate of change, thus providing more robust and efficient solutions for frequency regulation in hybrid systems.

Optimization algorithms play a critical role in tuning the parameters of controllers[30,31] to enhance system performance[32]. Traditional optimization techniques such as genetic algorithm (GA)[33], firefly algorithm (FA)[34], and salp swarm algorithm (SSA)[35,36] have been extensively applied to optimize LFC controllers. However, these methods often struggle with issues like local optima and slower convergence rates. In this research, we propose

the bio-dynamic grasshopper optimization algorithm (BDGOA), a novel optimization technique, to optimize the parameters of a newly developed multi-stage TDn(1 + PI) controller.

A variety of controllers have been developed for LFC in hybrid microgrids and interconnected power systems. Notably, traditional controllers like PI and PID are widely used due to their simplicity, but they often fall short in handling the nonlinear dynamics of hybrid systems[37]. To address these limitations, several multi-stage and fractional-order controllers have emerged. For instance, Shayeghi and Rahnama[38] introduced a multistage TDF(1 + FOPI) controller optimized using the bonobo optimization algorithm (BOA). The controller demonstrated superior dynamic performance, particularly in handling uncertainties and sudden load changes, when compared to conventional PI and PID controllers. Similarly, Shayeghi, et al.[39] presented a TFODn-FOPI controller, which outperformed standard controllers in islanded microgrid systems by reducing the detrimental effects of time-delay nonlinearities and cyber vandalism.

Optimization algorithms have played a critical role in enhancing the tuning of these controllers. Ekinci et al.[40] employed the RIME algorithm to optimize a PI controller for automatic generation control (AGC) in hybrid PV-reheat thermal systems, showcasing its effectiveness in reducing frequency oscillations and tie-line power changes. Moreover, Can and Ayas[41] introduced a GTO-based PI controller, which outperformed other optimization techniques like GA and SSA in terms of cutting down on settling times and overshoot values.

Among the most recent approaches, hybrid and intelligent control strategies have gained prominence. Haroun and Li[42] proposed a hybrid fuzzy logic intelligent PID (FLiPID) controller, optimized using particle swarm optimization (PSO), for boiler dynamics and physically constrained multi-area power systems that are interconnected (BDs). This approach improved the system's robustness and dynamic response compared to traditional methods. Additionally, they highlighted the potential of a FLiPID controller to manage LFC more effectively under nonlinear conditions.

In terms of novel optimization techniques, Khadanga, et al.[43] introduced an algorithm MWOA to design a PIDF controller for a two-area power system. The MWOA algorithm showed improvements in implementation time and solution quality over traditional whale optimization algorithm (WOA), further contributing to better frequency regulation in hybrid systems.

The performance of these various controllers and optimization techniques highlights the importance of choosing the right combination for specific system dynamics. A study by Arya[28], which focused on a multi-stage FPIDF-(1 + PI) controller for AGC, demonstrated that combining advanced control strategies with energy storage systems like capacitive energy storage (CES) units could significantly enhance system stability. Finally, Shayeghi and Rahnama[29] proposed a PD-(1 + PI) controller for an entirely renewable microgrid, emphasized the role of demand response programs (DRPs) in achieving robust performance under fluctuating RESs. The main findings from these recent studies are summarized in Table 1.

Research gap and motivation

Despite significant advancements in LFC strategies for hybrid power systems, several critical challenges remain. Most existing studies focus on either PV systems or thermal power plants independently, often neglecting the complex dynamic interactions between these energy sources in hybrid systems. Additionally, while optimization algorithms like GA, SSA, and FA have been extensively applied to tune LFC controllers, they often suffer from limitations such as slow convergence rates and vulnerability to local optima. These drawbacks hinder their performance in addressing the nonlinearities and uncertainties inherent in hybrid power systems, including governor deadband, boiler dynamics, and time delays.

Another gap lies in the lack of comprehensive evaluations of multi-stage controllers that effectively balance transient and steady-state performance in such systems. While multi-stage and fractional-order controllers have shown promise in improving robustness and dynamic responses, their application in hybrid PV-thermal power systems remains underexplored, particularly under nonlinear operating conditions and varying system parameters.

Motivated by these gaps, this research introduces a novel BDGOA to optimize a multi-stage TDn(1 + PI) controller for LFC in a two-area power system with PV and thermal generators. This approach aims to enhance system stability and reliability by addressing the aforementioned challenges, offering superior performance compared to conventional methods. The study evaluates the controller's robustness under diverse scenarios, including parameter uncertainties and nonlinearities, highlighting its practical applicability for modern power grids.

Contributions

This research offers several significant contributions to the area of LFC in power systems:

- **Development of a novel multi-stage controller**: The work presents a novel multi-stage TDn(1 + PI) controller specifically made for LFC in a two-area power system with a PV power plant and a reheat thermal generator. System stability and dynamic response are greatly increased by this controller's special blend of a PI controller and a TDn filter.
- **Analysis of the PV power plant's influence**: The effects of the PV power plant on frequency control under various operating situations are thoroughly examined in this study. Significant new information on the LFC system's performance and dynamic behavior with integrated renewable energy is provided by this analysis.
- **Superior performance of the proposed controller**: The newly developed multi-stage BDGOA-tuned TDn(1 + PI) controller is compared with several existing methods, such as MWOA-tuned PIDn[43], MWOA-tuned PID[43], RIME-tuned PI[40], BWOA-tuned PI[44], SSA-tuned PI[45], SFLA-tuned PI[46], FA-tuned PI[34], GA-tuned PI[34], GTO-tuned PI[41], and WOA-tuned PI[43] controllers from previous research. Results show that the

Article	Methodology	Multi-area	Non-linear Model	Uncertainty in Design	Uncertainty in Simulation	Primary Control	Secondary Control	Delay in Design	Delay in Simulation	Key Findings
Ref[37]	Modified sine cosine algorithm (MSCA) optimized multi-stage TDF/(1 + TI) controller for LFC	Yes	Yes	No	No	Tilt-derivative filter (TDF)	PI control	No	No	MSCA-based TDF/(1 + TI) controller outperforms PI and PID controllers in stabilizing frequency oscillations in microgrid systems
Ref[38]	BOA for optimizing multi-stage TDF(1 + FOPI) controller	Yes	Yes	Yes	Yes	Fractional-order proportional-integral (FOPI)	Yes	Yes	No	TDF(1 + FOPI) controller provides superior dynamic response in uncertain environments, reducing overshoot and time errors
Ref[39]	Prairie dog optimization (PDO) for tuning TFODn-FOPI controller for islanded microgrid	Yes	Yes	Yes	Yes	Tilt-fractional-order derivative (TFODn)	FOPI control	Yes	Yes	TFODn-FOPI controller effectively handles time delays, RES output fluctuations, and parameter uncertainties, outperforming traditional controllers
Ref[42]	PSO to optimize hybrid fuzzy logic intelligent PID (FLiPID) controller	Yes	Yes	Yes	Yes	Fuzzy logic with PID	Yes	No	Yes	FLiPID controller shows robust performance in multi-area systems with physical constraints and BDs
Ref[40]	RIME optimization algorithm to optimize PI controller for AGC	Yes	No	Yes	Yes	PI control	Yes	No	No	RIME-optimized PI controller reduces frequency oscillations and tie-line power changes more effectively than conventional methods
Ref[28]	Imperialist competition algorithm (ICA) for multi-stage FPIDF-(1 + PI) controller	Yes	Yes	No	Yes	Fuzzy logic PID with filter (FPIDF)	Yes	Yes	Yes	FPIDF-(1 + PI) controller with CES enhances frequency regulation in PV-thermal systems
Ref[29]	Particle swarm optimization with time-varying acceleration coefficients (PSO-TVAC) to optimize PD-(1 + PI) controller	No	Yes	Yes	Yes	Proportional-derivative (PD) with PI	Yes	No	Yes	PD-(1 + PI) controller improves dynamic response and reduces oscillations in entirely renewable microgrid systems
Ref[27]	SSA optimization for I-TD*N* control structure in interconnected hybrid power systems	Yes	Yes	Yes	Yes	Tilt-derivative integral (TD*N*)	Yes	Yes	No	I-TD*N* control structure outperforms PID and I-PD controllers in terms of performance and robustness against parameter variations
Proposed	Bio-dynamic grasshopper optimization (BDGOA) tuned multi-stage TDn(1 + PI) controller for LFC	Yes	Yes	Yes	Yes	Tilt-derivative with filter (TDn)	PI control	Yes	Yes	Multi-stage BDGOA-tuned TDn(1 + PI) controller effectively manages time delays and parameter uncertainties while reducing frequency oscillations and tie-line power fluctuations more efficiently than other commonly used methods.

Table 1. Overview of utilizing controller and optimization method in the recent paper.

BDGOA-tuned TDn(1 + PI) controller outperforms these controllers, demonstrating superior robustness and efficiency in frequency regulation.

- **Validation of robustness and contribution to system stability**: The research proves the robustness of the BDGOA-tuned TDn(1 + PI) controller under various complex operating conditions, including random and stepwise load changes, system parameter variations, and nonlinearities. The controller's ability to maintain stable performance in these diverse scenarios underscores its reliability and practical application, making it a powerful tool for enhancing overall system stability and ensuring a reliable energy supply in hybrid power systems.
- **Additional contributions**: The study also addresses critical nonlinear factors in LFC, including time delay (TD), governor deadband (GDB), and boiler dynamics (BD). While previous studies have explored the effects of GDB and BD in PV-thermal power systems[41], this research uniquely investigates the influence of TD as a nonlinear factor. By incorporating these elements, the study provides new insights and a more thorough understanding of LFC in PV-thermal power systems, further increasing the novelty and impact of the research.

Additionally, the paper is organized into six main sections: Sect. 1 offers an introduction, followed by Sect. 2, which presents and explains the specifics of the photovoltaic and thermal power system. In Sect. 3, the proposed TD*n*(1 + PI) controller is introduced and analyzed. Section 4 addresses the problem formulation and provides an overview of how the BDGOA optimization technique is integrated with the proposed controller. Section 5 presents the results of control strategy evaluations, various scenarios, and comparative analyses. Lastly, Sect. 6 concludes the paper and outlines potential future work.

Modelling of photovoltaic and thermal power system

A test model was used to evaluate the multi-stage TDn(1 + PI) controller's performance. This model integrates a PV system and reheat thermal system into a two-area power system. The PV system and its related loads make up Area 1 of Fig. 1, whereas the reheat thermal power system and its related loads make up Area 2.

The Eq. (1) represents the transfer function of the solar PV system in area-1, which includes the PV panel, maximum power point tracking (MPPT), converter, and filter.

$$G_{PV}(s) = \frac{A - Bs}{s^2 + Cs + D} = \frac{900?18s}{s^2 + 100s + 50} \tag{1}$$

The governor, turbine, reheater, and power system are located in Area 2. According to Eqs. (2)–(5), first-order systems are used to express the transfer functions for these components. In these equations, τ_G, τ_T, τ_R, τ_{PS} represent the time constants, while K_G, K_T, K_R, K_{PS} denote the respective gains for each component of the power system[34,40,41,43–48]. The transfer functions of the governor, turbine, reheater and power system are given respectively as:

$$G_G(s) = \frac{K_G}{1 + s\tau_G} = \frac{1}{1 + 0.08s} \tag{2}$$

$$G_T(s) = \frac{K_T}{1 + s\tau_T} = \frac{1}{1 + 0.3s} \tag{3}$$

$$G_R(s) = \frac{1 + sK_R\tau_R}{1 + s\tau_R} = \frac{1 + 3.3s}{1 + 10s} \tag{4}$$

$$G_{PS}(s) = \frac{K_{PS}}{1 + s\tau_{PS}} = \frac{120}{1 + 20s} \tag{5}$$

Variations in tie-line power and frequency variances are the sources of the area control error (ACE). For Area 1, it is stated in Eq. (6), and for Area 2, in Eq. (7). The ACE for Area 2 accounts for key factors, such as the frequency bias parameter (B) and the change in tie-line power ΔP_{tie}) between the two areas.

$$ACE_1 = \Delta P_{tie} \tag{6}$$

$$ACE_2 = B\Delta f_2 + \Delta P_{tie} \tag{7}$$

To properly evaluate how well the BDGOA-tuned TDn(1 + PI) controller works and make sure it is effective, we need to consider factors like nonlinearities, including GDB and BD, as well as TDs. The model of a two-area

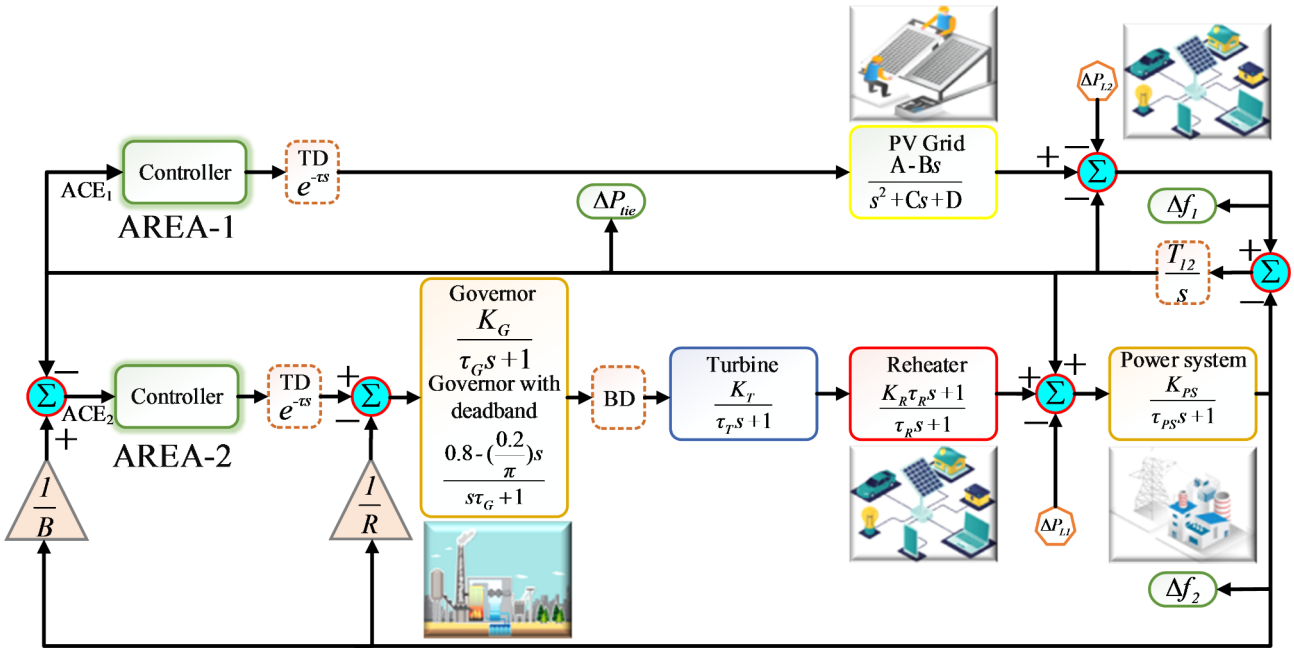


Fig. 1. Overview of two-area PV-thermal power system with nonlinearity.

PV-thermal power system with these components included is displayed in Fig. 1. In this figure, Δf_1 represents the frequency changes in area-1, Δf_2 represents the frequency changes in area-2, ΔP_{tie} shows the changes in power between the areas, and R is the regulation droop. The main goal of LFC is to reduce the overall frequency changes in each area and the power deviations between the areas.

The transfer function of GDB is detailed in Eq. (8). This study also investigates a different nonlinearity called BD, which denotes a device used for generating steam under pressure. Figure 2 illustrates the BD model and its component transfer functions, which are mathematically represented by Eqs. (9)-(11)[41,42].

$$G_{GDB}(s) = \frac{0.8 - \left(\frac{0.2}{\pi}\right)s}{1 + s\tau_G} = \frac{0.8 - \left(\frac{0.2}{\pi}\right)s}{1 + 0.08s} \tag{8}$$

The transfer functions of the pressure control, fuel system and boiler storage are given respectively as:

$$PC = \frac{K_{IB}T_{IB}s^2 + K_{IB}(T_{RB} + T_{IB})s + K_{IB}}{0.1T_{RB}s^2 + s} = \frac{0.78s^2 + 2.85s + 0.03}{6.9s^2 + s} \tag{9}$$

$$FS = \frac{e^{-T_d s}}{1 + T_F s} = \frac{1}{1 + 10s} \tag{10}$$

$$BS = \frac{1}{C_B s} = \frac{1}{200s} \tag{11}$$

Proposed multi-stage TD*n*(1 + PI) controller

The goal of the suggested multi-stage TDn(1 + PI) controller is to maximize the LFC in a two-area power system that consists of a PV power plant and a reheat thermal generator. This innovative design is structured into two stages, each of which contributes to different aspects of system performance, leading to enhanced dynamic response, frequency stability, and improved control over tie-line power oscillations.

In the first stage, the TD*n* controller focuses on refining the system's transient response, particularly in reducing the oscillations that occur during disturbances. The tilt-derivative aspect is a modification of the traditional derivative controller, which not only addresses the rate of change in error but also adjusts the slope of the error signal over time. This allows the system to respond more gradually and effectively to disturbances, preventing abrupt changes that might destabilize the system. By incorporating this tilt function, the controller reduces the amplitude of oscillations, which is crucial when dealing with the inherent fluctuations caused by RESs like PV systems. The inclusion of an N filter in this stage plays a vital role in smoothing out high-frequency noise in the system, which typically arises from the variability of PV power generation. This noise can interfere with control decisions, so filtering it out ensures that the controller reacts only to significant changes in system behavior, rather than responding to spurious signals. The overall effect of the TD*n* stage is a much smoother and more controlled transition during disturbances, reducing the risk of prolonged oscillations and allowing the system to return to stability more quickly.

The second stage of the controller involves the PI component, which is crucial for correcting both steady-state errors and providing a stable long-term response. The proportional action in this stage delivers an immediate reaction to any frequency deviation by producing a control signal proportional to the magnitude of the error. This helps in providing initial corrective actions as soon as any disturbance occurs, keeping the system from drifting too far from the desired set point. However, while the proportional action helps minimize the immediate deviation, it alone is insufficient to eliminate steady-state errors over time. This is where the integral action becomes critical. The integral part continuously accumulates the error over time and adjusts the control output to ensure that any persistent deviation from the desired frequency is corrected. This process ensures that the system reaches a stable operating point without residual frequency deviations. In combination, the PI controller ensures that both short-term and long-term errors are addressed, providing a balanced response that eliminates steady-state errors while maintaining system stability during dynamic conditions. The block diagram illustrating the proposed controller is depicted in Fig. 3.

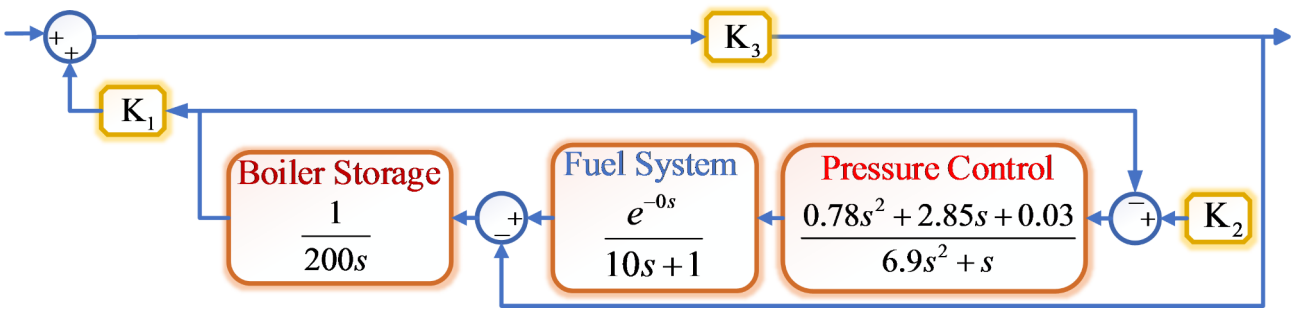


Fig. 2. Block diagram of the BD system.

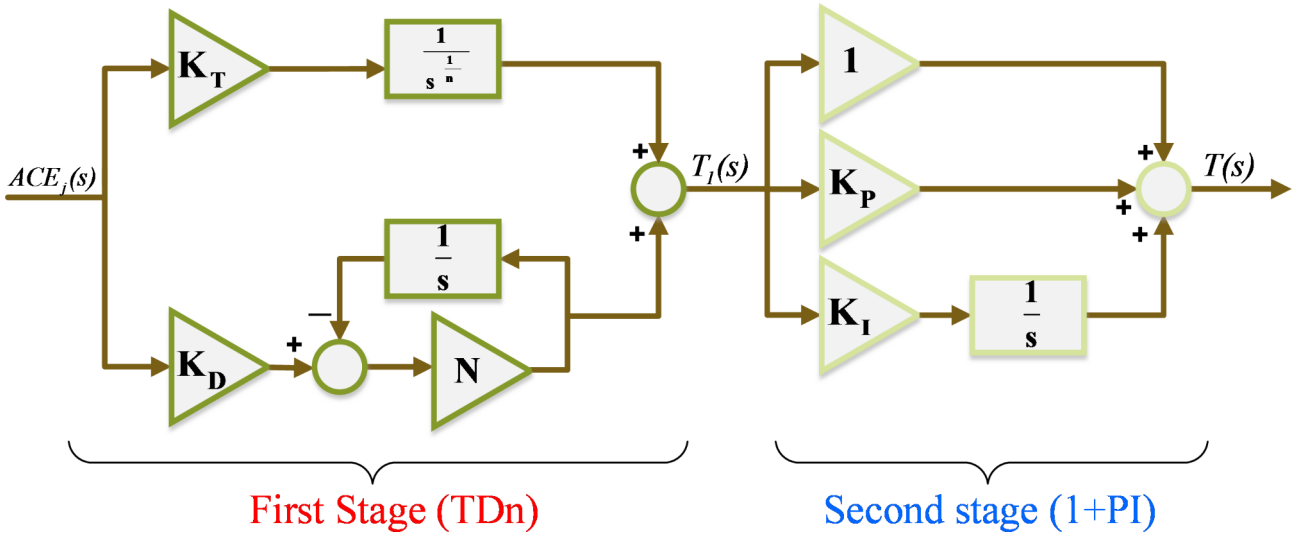


Fig. 3. Proposed TD*n*(1 + PI) controller structure.

By integrating these two stages, the TD*n*(1 + PI) controller provides a comprehensive solution that addresses both the dynamic and steady-state requirements of LFC. The TD*n* stage significantly reduces oscillations and improves the system's transient response by filtering out noise and managing the rate of change, which is essential in systems with RES prone to fluctuations. The PI stage ensures that steady-state errors are corrected and that the system maintains a stable frequency after disturbances. This multi-stage approach leads to a faster settling time, less oscillatory behavior, and improved long-term stability, making it an ideal solution for modern power systems that combine conventional and RESs. The combined effect of the TD*n* and PI stages enhances the overall performance of the system, providing faster, more stable, and more accurate LFC. The open-loop transfer function of the first stage controller is shown as Eq. (12):

$$G_{TDn}(s) = \frac{K_T}{s^{\frac{1}{n}}} + [K_D \times \left(\frac{Ns}{N+S}\right)] \tag{12}$$

The open-loop transfer function of the second stage controller is shown as Eq. (13):

$$G_{(1+PI)} = 1 + K_P + \frac{K_I}{s} \tag{13}$$

The open-loop representation of the proposed controller can be depicted by Eq. (14).

$$G_{TDn(1+PI)} = \left[\frac{K_T}{s^{\frac{1}{n}}} + \left(\frac{K_D N s}{N+s}\right)\right] \times \left[\frac{(1+K_P)\,s + K_I}{s}\right] \tag{14}$$

Finally, Eqs. (15)-(20) illustrate the closed-loop system.

$$G_{TDn(1+PI)} = \left[\frac{K_T \times (N+s) + K_D \times N \times s^{\frac{1}{n}} \times s}{(s+N) \times s^{\frac{1}{n}}}\right] \times \left[\frac{(1+K_P) \times s + K_I}{s}\right] \tag{15}$$

$$G_{TDn(1+PI)} = \frac{[K_T N + K_T s + K_D N s^{\left(\frac{1}{n}+1\right)}] \times (s + K_P s + K_I)}{(s+N) \times s^{\frac{1}{n}} \times s} \tag{16}$$

$$G_{TDn(1+PI)} = \frac{[K_T N s + K_T K_P N s + K_T K_I N + K_T s^2 + K_T K_P s^2 + K_T K_I s + K_D N s^{(2+\frac{1}{n})} + K_D K_P N s^{(2+\frac{1}{n})} + K_D K_I N s^{(1+\frac{1}{n})}]}{s^{(2+\frac{1}{n})} + N s^{(1+\frac{1}{n})}} \tag{17}$$

$$G_{TDn(1+PI)} = \frac{[(K_D N + K_D K_P N)\, s^{(2+\frac{1}{n})} + K_D K_I N s^{(1+\frac{1}{n})} + (K_T + K_T K_P) s^2 + (K_T N + K_T K_P N + K_T K_I)\, s + K_T K_I N]}{s^{(2+\frac{1}{n})} + N s^{(1+\frac{1}{n})}} \tag{18}$$

If we substitute the optimal parameters of BDGOA-TDn(1 + PI) controller, given in Table 2, into Eq. (18), the following will be obtained.

$$G_{TDn(1+PI)_{Area-1}} = -\frac{((5.0701E+03)s^{75.5294} + (1.9129E+03)s^{74.5294} + 3.9s^2 + 5.0716(E+03)s + 1.9129E+03)}{1s^{75.5294} + 1.3E^{+3}s^{74.5294}} \tag{19}$$

$$G_{TDn(1+PI)_{Area-2}} = -\frac{((2.2346E+03)s^{420.9359} + 2.1994(E+03)s^{419.9359} + 3.9156s^2 + 4.7028(E+03)s + 4.6250E+03)}{1s^{420.9359} + 1.2001E^{+3}s^{419.9359}} \tag{20}$$

Controller-Algorithm	Area	Parameters							
		K_T	K_D	K_P	K_I	λ	μ	N	n
BDGOA-TDn(1 + PI) (Proposed)	Area1	-2	-2	0.95	0.7357	1	1	1300.0342	0.0136
	Area2	-2	-0.951089	0.9578	1.927	1	1	1200.0614	0.002387
BDGOA-FOPID	Area1	0	-1.5916	-2	-2	1	0.8516	0	0
	Area2	0	-2	-2	-2	0.9605	0.2326	0	0
MWOA-PIDn[43]	Area1	0	-1.5383	-1.9117	-0.0649	1	1	0	5.5236
	Area2	0	-0.1417	-1.8875	-1.3179	1	1	0	5.5236
MWOA-PID[43]	Area1	0	-0.6112	-0.1070	-0.0906	1	1	0	0
	Area2	0	-0.2505	-1.8938	-1.8935	1	1	0	0
BDGOA-PID	Area1	0	-0.0415	-0.45397	-0.093464	1	1	0	0
	Area2	0	-0.3853	-1.05	-0.94357	1	1	0	0
BDGOA-PI	Area1	0	0	-1.7121	-0.1126	1	0	0	0
	Area2	0	0	-2	-0.9732	1	0	0	0
RIME-PI[40]	Area1	0	0	-0.45397	-0.093464	1	0	0	0
	Area2	0	0	-2	-0.94357	1	0	0	0
BWOA-PI[44]	Area1	0	0	-0.66708	-0.54768	1	0	0	0
	Area2	0	0	-2	-0.84696	1	0	0	0
SSA-PI[45]	Area1	0	0	-0.7715	-0.0483	1	0	0	0
	Area2	0	0	-1.0837	-0.8929	1	0	0	0
SFLA-PI[46]	Area1	0	0	-0.5156	-0.9012	1	0	0	0
	Area2	0	0	-0.7896	-0.8965	1	0	0	0
FA-PI[34]	Area1	0	0	-0.8811	-0.5765	1	0	0	0
	Area2	0	0	-0.7626	-0.8307	1	0	0	0
GA-PI[34]	Area1	0	0	-0.5663	-0.4024	1	0	0	0
	Area2	0	0	-0.5127	-0.7256	1	0	0	0
GTO-PI[41]	Area1	0	0	-0.5235	-0.0973	1	0	0	0
	Area2	0	0	-2	-0.9238	1	0	0	0
WOA-PI[43]	Area1	0	0	-0.4563	-0.2254	1	0	0	0
	Area2	0	0	-0.8967	-0.9865	1	0	0	0

Table 2. Optimum gains of proposed and other controllers.

Additionally, an overview of the PV-thermal power system and the proposed controller in two-area studied in this research is depicted in Fig. 4.

Optimization method

The bio-dynamic grasshopper optimization algorithm (BDGOA) is a modified version of the grasshopper optimization algorithm (GOA) which has been designed to improve the GOA performance in solving the difficult optimization problems. BDGOA addresses the major weaknesses of the original GOA such as, it has a tendency to get stuck in local minima and its convergence rate is slow. Through the introduction of new mechanisms and parameters, BDGOA strikes a better equilibrium between exploration and exploitation. The original GOA is a population-based optimization algorithm inspired by the natural behavior of grasshoppers, particularly their swarming behavior. In GOA, grasshoppers move in the search space under the influence of three main forces: social interaction, gravity, and wind advection. The combination of these forces helps the algorithm find the best solution to a given optimization problem. GOA is divided into two phases:

- **Exploration phase**: Grasshoppers move across the search space in large steps to explore different regions.
- **Exploitation phase**: Grasshoppers focus on smaller, refined movements to fine-tune their search in areas where promising solutions have been found.

However, despite its potential, GOA suffers from issues like getting stuck in local minima and an imbalanced focus on exploitation too early in the optimization process. This is where BDGOA comes into play. To overcome the limitations of GOA, the BDGOA introduces several enhancements that improve the overall performance of the optimization process. These improvements include:

- **Elimination and replacement mechanism**: One of the critical issues in GOA is that poor-performing grasshoppers can slow down the algorithm's ability to converge to the global best solution. BDGOA addresses this by periodically eliminating a percentage of the worst-performing grasshoppers after a specified number of iterations. These eliminated grasshoppers are replaced with new grasshoppers, which are randomly distributed in the search space. This not only refreshes the population but also helps avoid premature convergence by introducing new potential solutions.

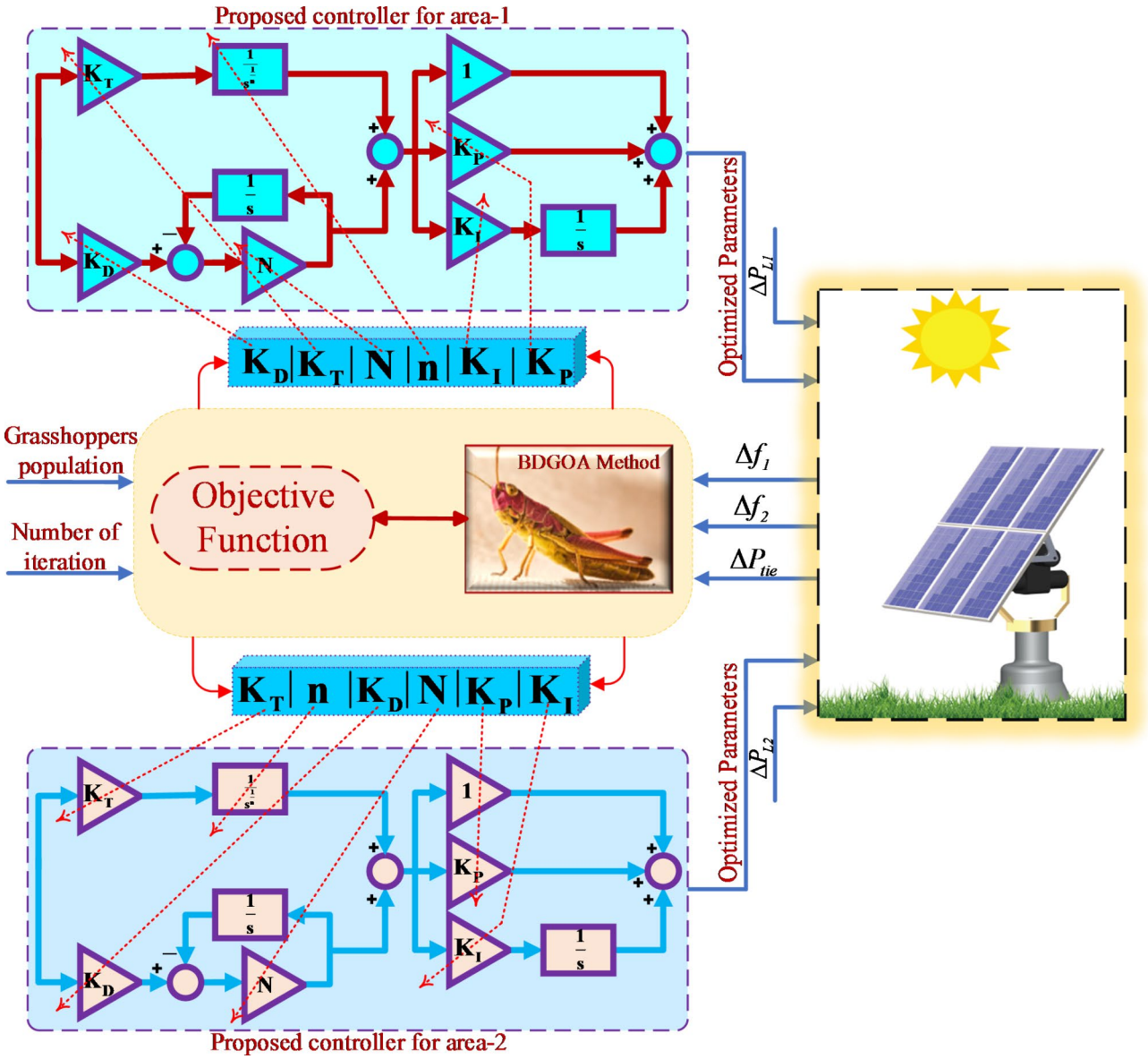


Fig. 4. General scheme of the under-examination model.

- **Adaptive search space expansion**: BDGOA dynamically adjusts the search space as the optimization process progresses. In the early stages, the search space may be relatively confined, allowing for focused exploration of promising regions. However, as the number of iterations increases and certain conditions are met, the search space expands. This gradual expansion helps ensure that the algorithm doesn't miss out on global solutions by restricting itself to a limited search area. The expansion rate is controlled by the parameter ω , which dictates how quickly the search space grows.
- **Exploration-exploitation balance**: One of the key challenges in any optimization algorithm is finding the right balance between exploration and exploitation. In BDGOA, this balance is achieved by controlling the rate at which the exploration diminishes and exploitation intensifies. The parameter ccc, which controls this balance, starts with a high value, emphasizing exploration, and gradually decreases over time, allowing the algorithm to focus more on exploitation in the later stages. This helps the algorithm explore new areas early on and refine the best solutions as it nears completion.

Selecting Parameters in BDGOA involves several key factors. The elimination percentage e_p defines the proportion of grasshoppers removed during each elimination phase, while the elimination threshold e_t specifies the number of iterations after which this phase occurs. The threshold for search space expansion T_h dictates when the algorithm starts expanding the search space to explore larger regions, and the search space growth rate ω controls how quickly the search space expands over time, allowing the algorithm to cover more ground as iterations progress. The BDGOA follows a structured process to solve optimization problems. It begins with initialization, where the objective function (OF) and constraints are defined, and a randomly

generated population of grasshoppers represents potential solutions. In the fitness evaluation step, each grasshopper's position is assessed based on the OF to determine its fitness. The grasshopper positions are then updated using the GOA equation, influenced by factors like social interaction, gravity, and wind forces. After a specified number of iterations, the elimination and replacement phase occur, where the worst-performing grasshoppers are removed and replaced by new ones to maintain diversity and prevent premature convergence. As the algorithm progresses, once a predefined threshold is reached, the search space expands, controlled by the parameter ω, allowing the grasshoppers to explore larger areas of the solution space and increasing the likelihood of finding the global optimum. The algorithm iterates through these steps until the maximum number of iterations is reached, continuously updating the best solution. Finally, once the termination criteria are met, the algorithm outputs the best solution found. Table 3 show all steps in optimization process. Figure 5 depicts the schematic of the proposed controller utilizing the BDGOA optimization method in PV-thermal power system.

4.1 Objective function definition

The objective function (OF) is a tool used by designers to assess how the system responds dynamically. It aims to guarantee that the control mechanism's output delivers the best performance across different operating conditions, specifically targeting the minimization of steady-state error. This study aims to carefully adjust the TDn(1 + PI) controller settings using an optimization method called BDGOA to reduce fluctuations in frequency and tie-line power in power systems that include RES. So, OF employed is the ITAE, defined by Eq. (21)[40,41].

$$OF_{min} = \int_0^{t_{sim}} t(|\Delta f_1| + |\Delta f_2| + |\Delta P_{tie}|)dt \tag{21}$$

Here, t and t_{sim} are present and simulation time, respectively. The OF is restricted by the range of controller coefficients, defining the search space for the optimization problem as presented in Table 4.

The BDGOA optimization algorithm was executed in 30 separate rounds, with Table 5 displaying the best, worst, average, and standard deviation (SD) of OF values achieved by different controllers. In addition to the displayed values, the BDGOA has a p-value of $1.7344E-06$ (obtained from Wilcoxon test[49–51]) with respect to all algorithms (BDGOA vs. GEO, BDGOA vs. GOA, BDGOA vs. PSO, BDGOA vs. POA), indicating its superiority.

Figure 6 compares the effectiveness of five algorithms: BDGOA, golden eagle optimization (GEO), GOA, pelican optimization algorithm (POA), and PSO in minimizing the OF, using boxplots. The boxplot in Fig. 6 clearly shows that the worst result from the BDGOA algorithm is significantly better than the best results from the other four algorithms, highlighting the superior performance of the BDGOA algorithm.

The BDGOA algorithm has been run for enough iterations to ensure it converges to the optimal point. We use the BDGOA technique to assess the effectiveness of the proposed controller. Figure 7 shows the results of this optimized approach, which reaches the lowest OF values after 50 iterations, demonstrating the controller's superior performance.

Finally, Table 2 shows the optimal controller parameter values in two-area obtained from the best results produced by the BDGOA algorithm.

For a comprehensive numerical comparison, calculations and reports on time-domain evaluation metrics were conducted across various scenarios. These metrics include the integral of square error (ISE), integral of time-weighted square error (ITSE), integral of absolute error (IAE), and integral of time-weighted absolute error (ITAE). The corresponding equations for these metrics are presented in Eqs. (22)-(25).

Bio-dynamic grasshopper optimization algorithm (BDGOA)
Problem Information Input: 1. Define the OF and constraints of the optimization problem. **Initialize Population**: 2. Randomly generate the initial population of grasshoppers with N members. **Fitness Evaluation**: 3. Calculate the fitness of each grasshopper based on the OF. **Update Grasshopper Position**: 4. Update each grasshopper's position using the GOA position update equation, influenced by social interaction, gravity, and wind. **Fitness Calculation and Best Solution Update**: 5. Recalculate the fitness of each grasshopper and update the best solution found so far. **Elimination Phase Check**: 6. After reaching the elimination threshold e_t, check if the number of iterations is a multiple of e_t. **Eliminate and Replace Grasshoppers**: 7. Eliminate a percentage e_P of the worst-performing grasshoppers and replace them with randomly generated grasshoppers. **Search Space Expansion**: 8. Expand the search space after a certain condition is met, with the growth rate controlled by ω, allowing exploration of a larger area. **Iteration Loop**: 9. Repeat the process until the termination criteria (maximum number of iterations T) are met. **Output Best Solution**: 10. Display the best solution found by the BDGOA.
End of BDGOA

Table 3. BDGOA steps in optimization process.

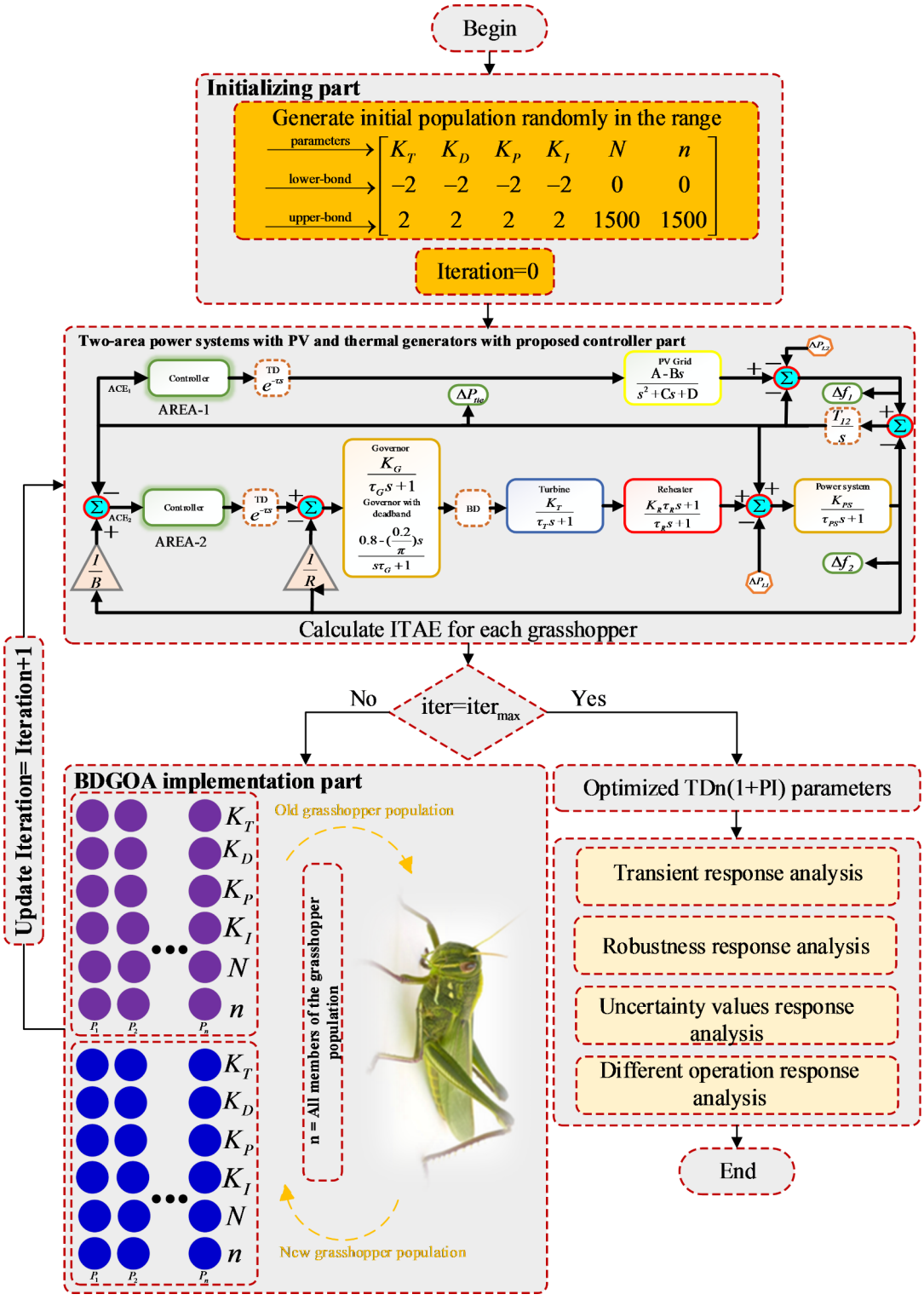


Fig. 5. The schematic of the proposed controller utilizing the BDGOA optimization method in PV-thermal power system.

Gains	K_T	K_D	K_P	K_I	N	n
Lower limit(min)	-2	-2	-2	-2	0	0
Upper limit(max)	2	2	2	2	1500	1500

Table 4. Range of gains in proposed and other controllers.

Algorithm	BDGOA×10^{-11}	GEO×10^{-11}	GOA×10^{-10}	PSO×10^{-9}	POA×10^{-9}
Best	1.162	7.201	7.573	8.321	9.685
Worst	4.776	9.478	10.574	15.347	13.902
Mean	2.213	9.010	10.485	14.121	11.858
SD	1.5663	0.9108	1.0570	21,990	1.8579

Table 5. Values of the OF following 20 rounds of optimization algorithms using TDn(1 + PI) controller.

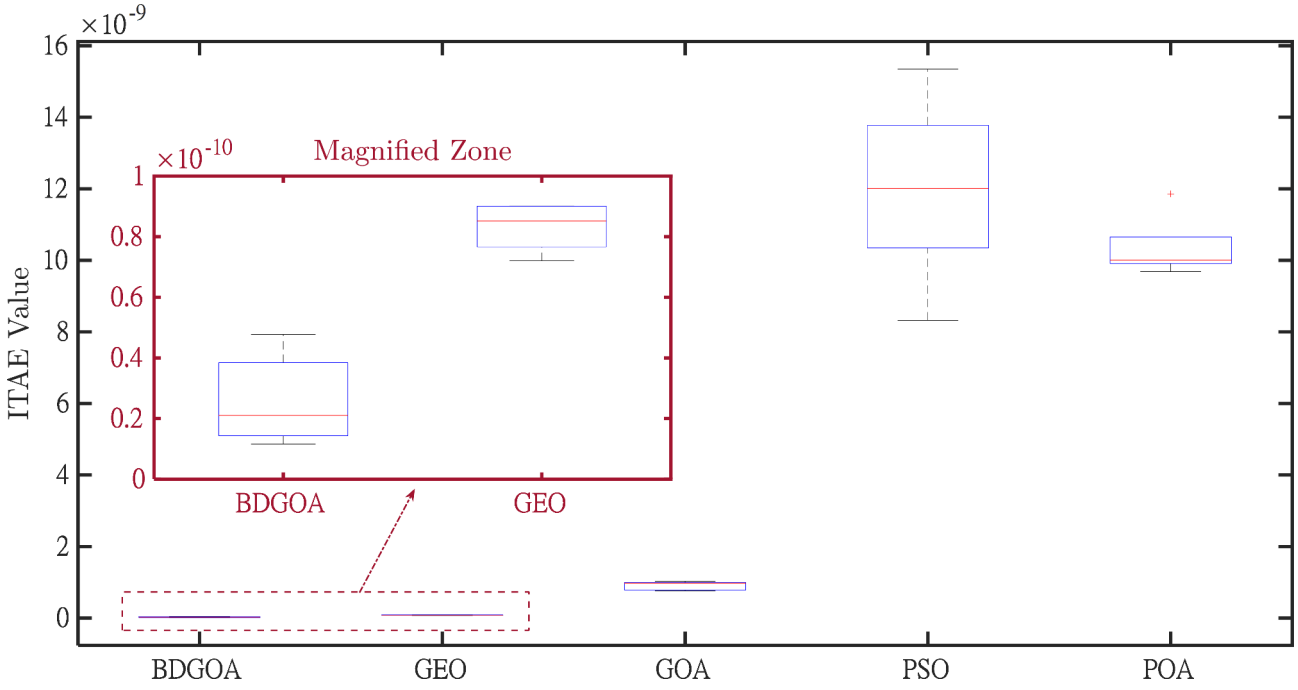


Fig. 6. Boxplots of BDGOA, GEO, GOA, PSO and POA algorithms using TDn(1 + PI) controller.

$$ISE = \int_0^x \left[(\Delta f_1)^2 + (\Delta f_2)^2 + (\Delta P_{tie})^2\right] .dt \tag{22}$$

$$ITSE = \int_0^x t. \left[(\Delta f_1)^2 + (\Delta f_2)^2 + (\Delta P_{tie})^2\right] .dt \tag{23}$$

$$IAE = \int_0^x (|\Delta f_1| + |\Delta f_2| + |\Delta P_{tie}|) .dt \tag{24}$$

$$ITAE = \int_0^x t. (|\Delta f_1| + |\Delta f_2| + |\Delta P_{tie}|) .dt \tag{25}$$

Parameter sensitivity analysis

The performance of the BDGOA is highly influenced by the choice of key parameters, particularly the iteration number and population size. These parameters were systematically analyzed in this study to determine their optimal values for LFC in hybrid power systems. An increase in iteration numbers or population size allows the algorithm to explore the search space more extensively. While this can enhance the chances of finding a global optimum, it comes at the cost of increased computational time. Our experiments show that beyond a certain

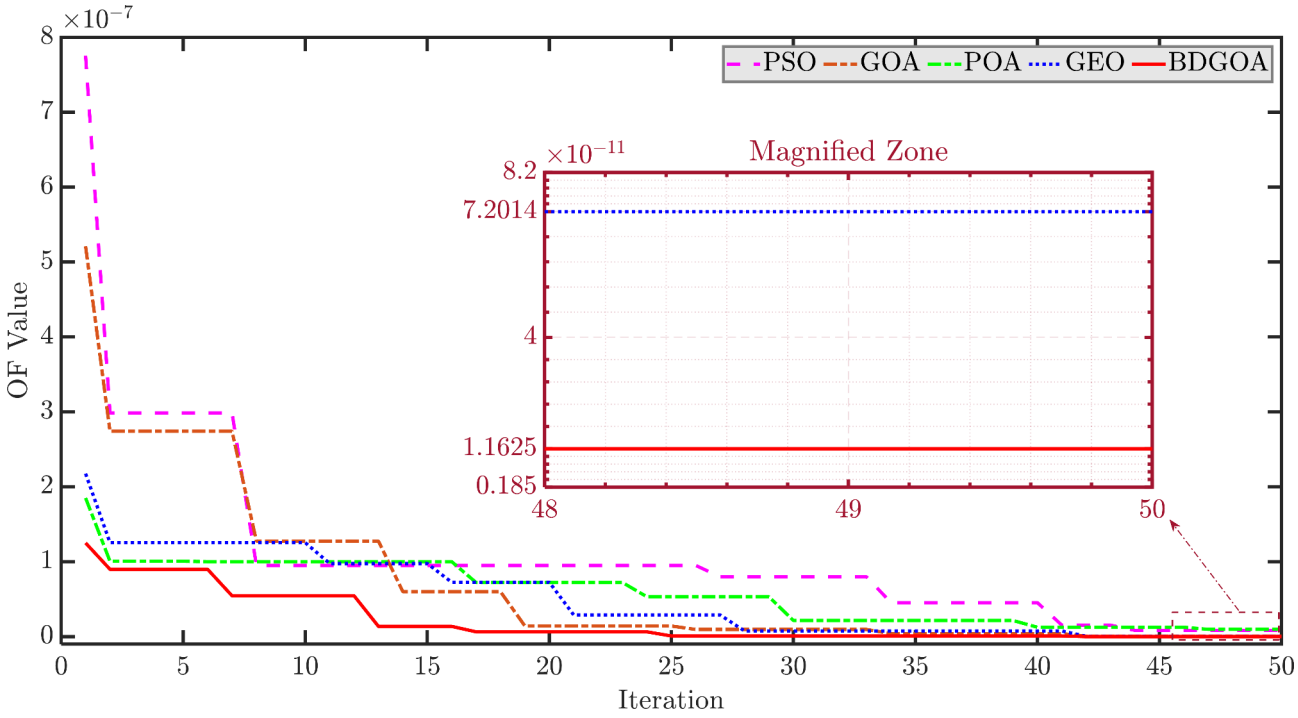


Fig. 7. Convergence profiles of BDGOA, GEO, GOA, PSO and POA algorithms using TDn(1 + PI) controller.

threshold, further increases in these parameters provide diminishing returns in terms of solution quality, while significantly escalating computational overhead.

Reducing the iteration number or population size below the optimal values limits the algorithm's ability to sufficiently explore and exploit the search space. This results in suboptimal tuning of the controller parameters, adversely affecting the stability performance of the LFC system. Specifically, inadequate exploration can lead to convergence towards local optima, undermining the algorithm's robustness in handling system nonlinearities and uncertainties.

To strike a balance, the optimal values of iteration numbers and population size were identified through rigorous trials. These values ensure that the BDGOA achieves high-quality solutions with minimal computational resources. The selected parameters allow for effective convergence within a reasonable time while maintaining the robustness and efficiency of the LFC system.

Simulation and analysis

In this section, the proposed TDn(1 + PI) controller is operationalized and integrated into the PV-thermal power system control mechanism as discussed earlier in Sect. 4. Moreover, these findings show a strong correlation between the results obtained from classical controllers. Subsequently, the closed-loop system is implemented using MATLAB 2023a with Simulink. Using 50 iterations and participation of 20 particles, the BDGOA algorithm effectively identifies the optimal controller coefficient values. The duration of the simulation is 30 s. Although we experimented with higher order approximations, they didn't significantly alter the results when evaluated in MATLAB. In this system, the parameters are set as follows[34,40,41,43–48]: $K_{PS} = 120$ Hz/pu.MW, $\tau_{PS} = 20$ s, $\tau_R = 10$ s, $\tau_G = 0.08$ s, $\tau_T = 0.3$ s, $K_R = 0.33$ Hz/pu.MW, $2\pi T_{1,2} = 0.54$ pu.MW / Hz, $B = 0.8$ pu.MW / Hz, $R = 2.5$ Hz/pu.MW

Analyzed PV-thermal power system in different operation

This section uses simulation experiments to assess the BDGOA-TDn(1 + PI) controller's performance in various settings. The system's reaction to load variations in the thermal system demand is evaluated in the first scenario. The behavior of the system is examined for variations in load in both regions in the second scenario. The system is then evaluated by increasing the load in Area 2 step-by-step before both regions see random load variations. The system's performance is then assessed while taking the power system's nonlinearities into account. Lastly, the system is assessed using several parameter values; Table 6 has a list of the pertinent BD parameters[41,42].

Scenario I: 10% step change in thermal system demand

In the first scenario, involving a 10% step change $(\Delta P_{D1} = 0.1\ pu)$ in thermal system demand, the system's response to a 0.1 pu load change at 0 s is analyzed. The resulting figures compare the proposed controller with the PI, PID, PIDn, FOPID controllers, focusing on frequency variations in area-1 (Δf_1), frequency variations in area-2 (Δf_2), and tie-line power variations (ΔP_{tie}). These comparisons are illustrated in Figs. 8, 9, 10, 11, 12 and 13 respectively. Tables 7 and 8 present detailed numerical data derived from the graphical representations.

Parameter	Value	Parameter	Value	Parameter	Value
K_1	0.85	C_B	200 s	K_{IB}	0.03
K_2	0.095	T_d	0 s	T_{IB}	26
K_3	0.92	T_F	10 s	T_{RB}	69 s

Table 6. Parameters of the boiler dynamic.

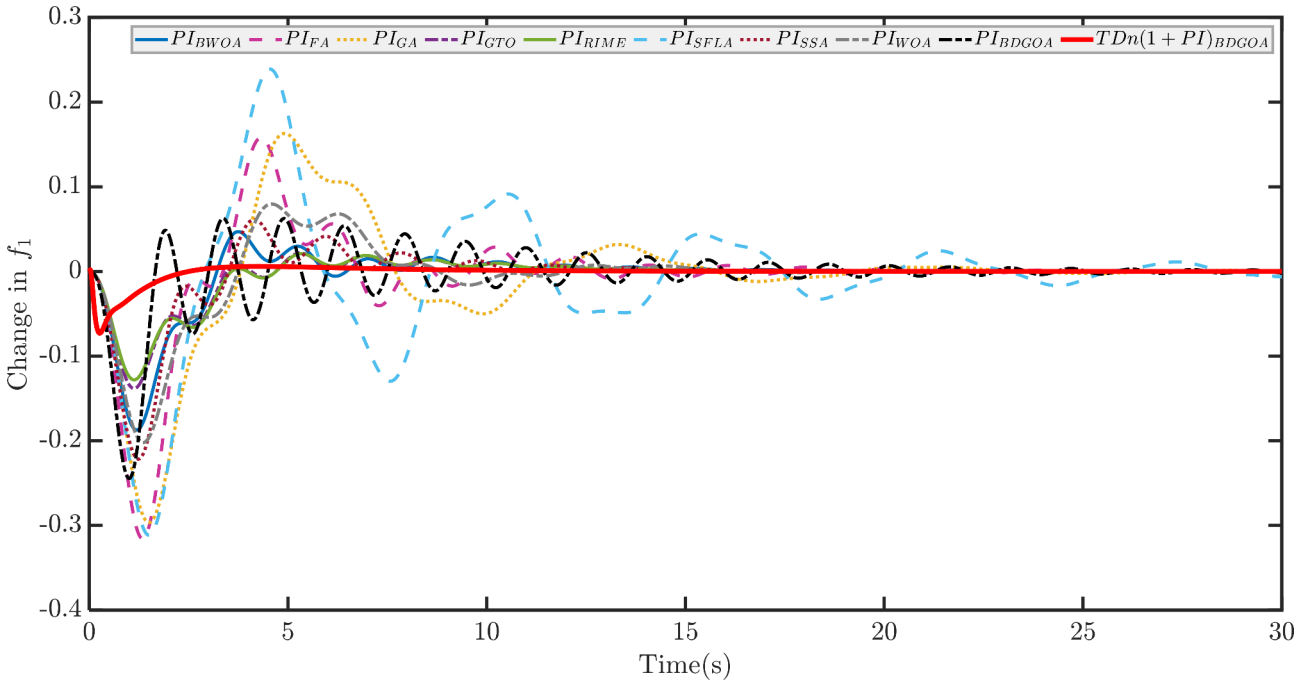


Fig. 8. Comparison of frequency variation Δf_1 for proposed and PI controllers in scenario I

Scenario II: both locations see a 10% step change

In the second scenario, which involves a 10% step change ($\Delta P_{D1} = 0.1\ pu$ and $\Delta P_{D2} = 0.1\ pu$) in both areas, the system's response to a 0.1 *pu* load change at 0s is analyzed. The resulting figures compare the proposed controller with the PI, PID, PID*n*, FOPID controllers focusing on frequency variations in area-1 (Δf_1), frequency variations in area-2 (Δf_2), and tie-line power variations (ΔP_{tie}). These fluctuations are depicted in Figs. 14, 15, 16, 17, 18 and 19 respectively. Tables 9 and 10 present detailed numerical data derived from the graphical representations.

Scenario III: stepwise load increase in area 2

The effectiveness of the suggested BDGOA-TDn(1 + PI) controller was assessed in Scenario III with notable variations in load, from 0.1 to 0.5 pu. The simulation results, displayed in Figs. 20 and 21, and 22, demonstrate how well the BDGOA-TDn(1 + PI) controller efficiently reduced the effects of sudden changes in load and rapidly reduced oscillations in both frequency and tie-line power deviations. These results highlight how well the controller keeps the system stable and guarantees dependable performance even in the face of significant load changes.

Scenario IV: both locations see a random load change

This part looks at the dynamics of the system in two different areas under various load circumstances. Figures 23 and 24, and 25 show how the system reacts to combined load variations of 0.05 pu, 0.1 pu, 0.2 pu, 0.3 pu, and 0.5 pu in Area 1 and Area 2. The convergence of oscillation patterns is demonstrated by these images, which also display the frequency fluctuations, and tie-line power variations brought on by synchronized load disturbances in the two sectors. Crucially, a quick and efficient damping reaction is indicated by the oscillations' quick reduction.

Scenario V: non-linear time-delay with random load variation in both locations

In this section, we examine the effects of sudden load changes in both areas, taking into account the impact of time-delay as a non-linearity factor on system dynamics. The system's responses to these abrupt load variations are presented, highlighting how TDs as a non-linearity factor affect overall performance. In this scenario, it is presumed that the control system's stimulation signal experiences a 20ms delay on both area controllers. The

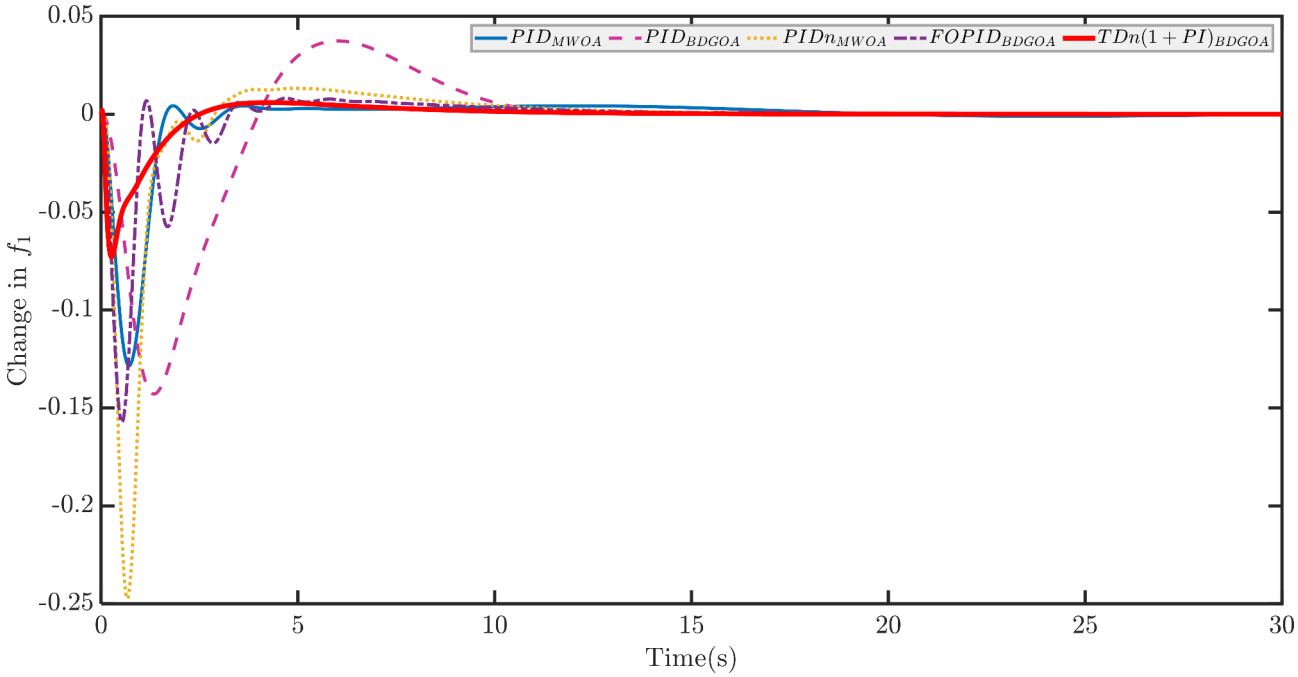


Fig. 9. Comparison of frequency variation Δf_1 for proposed and PID, PIDn and FOPID controllers in scenario I.

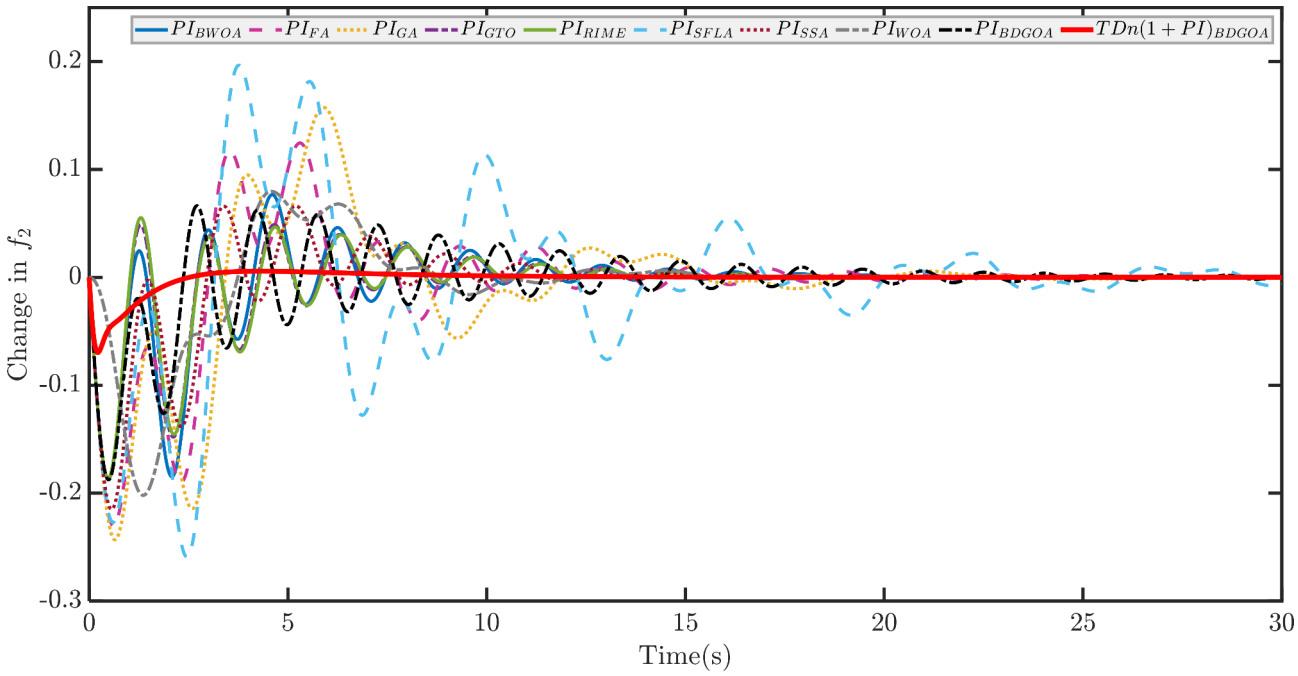


Fig. 10. Comparison of frequency variation Δf_2 for proposed and PI controllers in scenario I

results in Figs. 26, 27 and 28 show significant changes in frequency and tie-line power, demonstrating that TDs can increase oscillations and make system stabilization more difficult. Although the system eventually stabilizes, the presence of time-delay non-linearity slows down the damping process, resulting in longer-lasting oscillations before the system reaches stability. However, the proposed controller effectively overcomes these challenges, significantly improving system stability and damping oscillations more quickly.

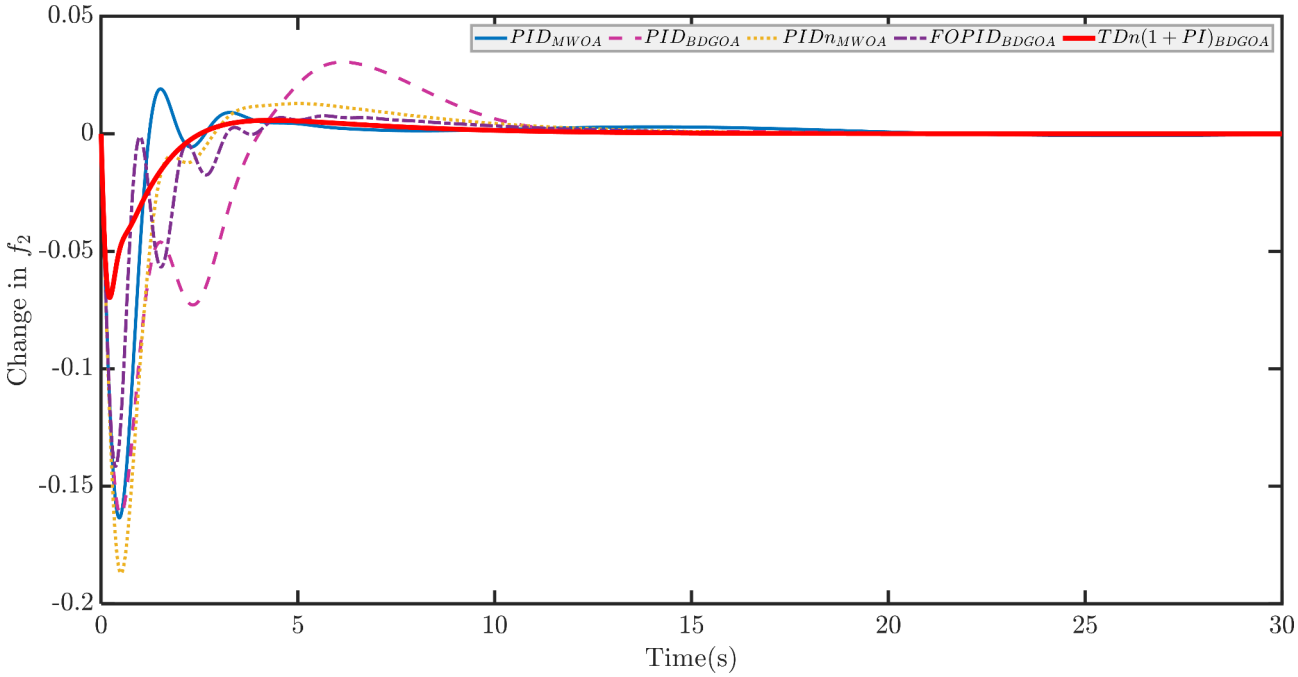


Fig. 11. Comparison of frequency variation Δf_2 for proposed and PID, PIDn and FOPID controllers in scenario I.

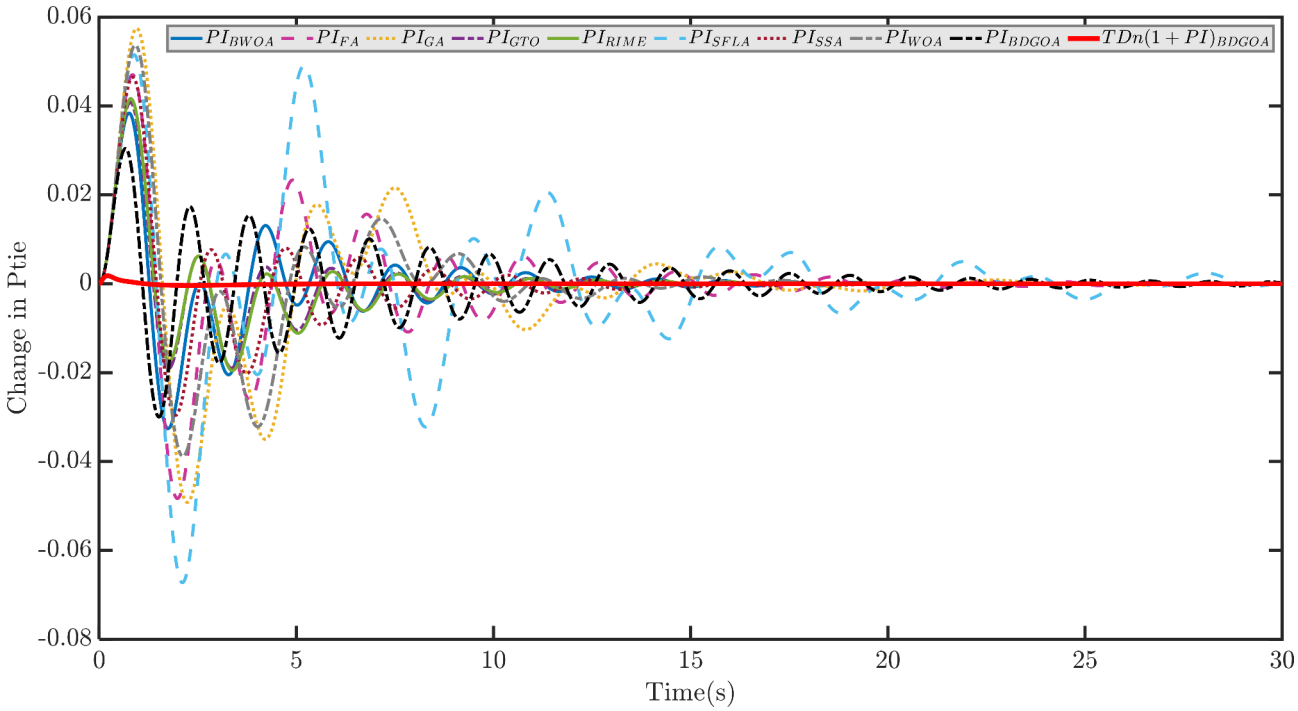


Fig. 12. Comparison of tie-line power deviation ΔP_{tie} for proposed and PI controllers in scenario I

Scenario VI: GBD and BD as nonlinearities

The behavior of the system was assessed when there are nonlinearities, such as boiler dynamics (BD) and governor deadband (GDB), to offer a more realistic analysis. When GDB is included, the oscillations in Area 1, Area 2, and the tie-line power deviations are shown in Fig. 29; the oscillations affected by BD are shown in Fig. 30. These graphs show that the tie-line power variations and frequency oscillations of the system are rapidly muted and remain within the specified bounds. In Fig. 31, where both BD and GDB are applied simultaneously,

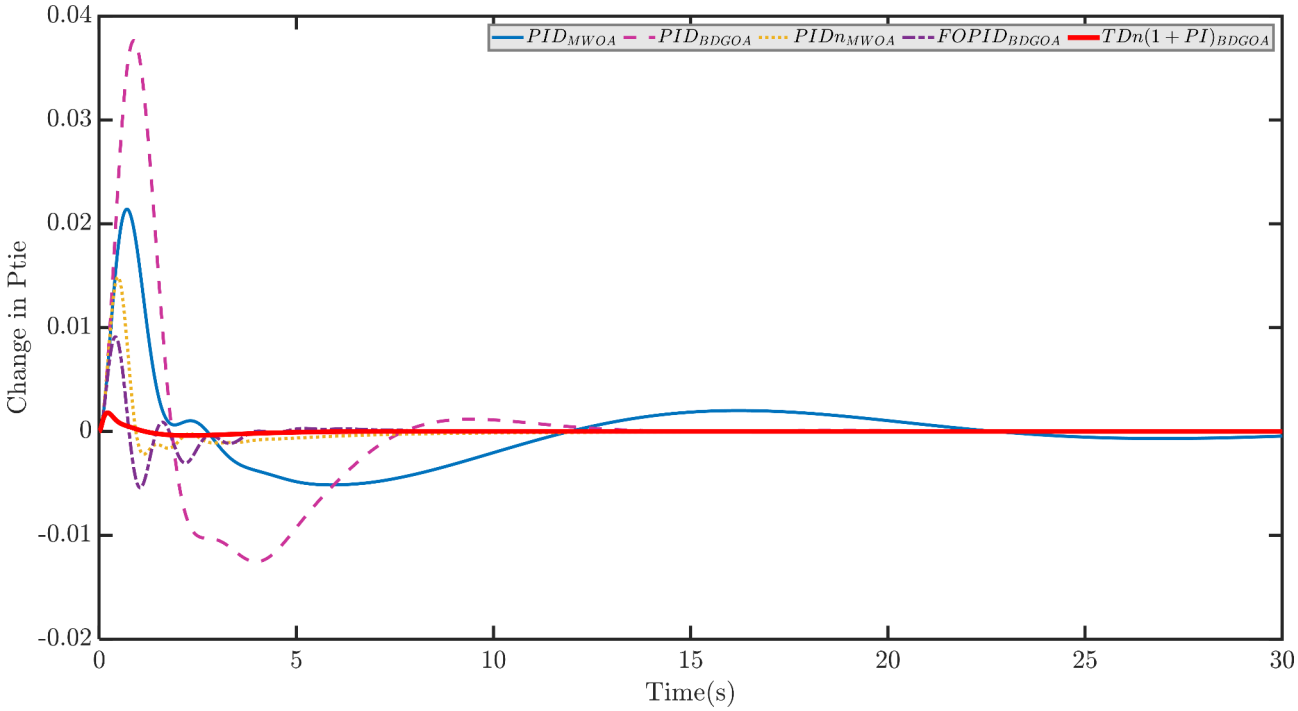


Fig. 13. Comparison of tie-line power deviation ΔP_{tie} for proposed and PID, PID*n* and FOPID controllers in scenario I.

	Δf_1				Δf_2				ΔP_{tie}			
Algorithm-Controller	**ST (s)**	**US**	**OS**	**TP (s)**	**ST (s)**	**US**	**OS**	**TP (s)**	**ST (s)**	**US**	**OS**	**TP (s)**
BDGOA-TD*n*(1 + PI) (Proposed)	0	-0.073035	0.0059617	4.2552	0	-0.069717	0.0057511	4.3112	0	-0.00038582	0.0018043	0.21449
BDGOA-FOPID	0.75987	-0.15731	0.0081675	4.6938	0.57391	-0.14152	0.007674	5.6738	0	-0.0054177	0.0091183	0.41536
MWOA-PID*n*[43]	1.0491	-0.2473	0.0132	4.9600	0.9825	-0.1870	0.0129	5.0200	0	-0.0022	0.0149	0.4800
MWOA-PID[43]	0.9831	-0.1284	0.0043	1.8300	0.8073	-0.1634	0.0191	1.5100	0	-0.0051	0.0214	0.7000
BDGOA-PID	2.1187	-0.1429	0.0375	6.0129	0.9471	-0.1621	0.0305	6.1429	1.3081	-0.0125	0.0376	0.8850
BDGOA-PI	1.4460	-0.2445	0.0626	3.3689	2.0807	-0.1876	0.0663	2.7130	1.6788	-0.0300	0.0304	0.6720
RIME-PI[40]	1.5072	-0.12799	0.020916	5.3391	2.4135	-0.18612	0.055346	1.2999	1.1359	-0.019541	0.041653	0.8020
BWOA-PI[44]	1.8198	-0.18722	0.047009	3.7467	2.4513	-0.18671	0.076656	4.6030	1.9896	-0.032573	0.038398	0.7620
SSA-PI[45]	1.8641	-0.22156	0.061433	4.1482	2.6092	-0.21499	0.06663	5.2023	2.1262	-0.029649	0.046477	0.8479
SFLA-PI[46]	7.9355	-0.31152	0.23905	4.5486	10.2501	-0.25917	0.19663	3.7690	8.5916	-0.067258	0.051529	0.8820
FA-PI[34]	4.8247	-0.31541	0.15791	4.3272	5.6017	-0.23017	0.12456	5.3064	3.9307	-0.048328	0.047025	0.8520
GA-PI[34]	6.6537	-0.29645	0.16298	4.9156	6.4543	-0.24313	0.15741	5.8994	4.5750	-0.049178	0.057467	0.9520
GTO-PI[41]	1.5515	-0.1382	0.0218	5.3192	2.4046	-0.1863	0.0489	4.6611	1.1134	-0.0191	0.0408	0.7920
WOA-PI[43]	2.1092	-0.2020	0.0797	4.5855	2.9217	-0.2212	0.0999	5.6420	4.3315	-0.0388	0.0536	0.9120

Table 7. Numerical results of ST, US, OS and TP for Δf_1, Δf_2, ΔP_{tie} in scenario I

the results confirm that the system remains stable, with the controller effectively handling the more complex nonlinear dynamics. This underscores the effectiveness of the BDGOA-TDn(1 + PI) controller in attenuating oscillations despite the presence of nonlinearities, highlighting its robustness in managing system dynamics and maintaining stability.

Scenario VII: fluctuation in parameters

In electrical power systems, sensitivity analysis is essential for anticipating system behavior in unpredictable circumstances and guaranteeing optimal functioning. In this study, a sensitivity analysis was conducted on the power system to evaluate performance under varying conditions. The governor, turbine, reheater, and power system components had their time constants adjusted by ± 25% as part of the analysis. The outcomes, which are shown in Figs. 32 and 33, and 34, show that the suggested controller was able to manage these fluctuations and

Algorithm-Controller	IAE	ISE	ITAE	ITSE
BDGOA-TDn(1 + PI) (Proposed)	0.1977	0.0057698	0.55392	0.0043688
BDGOA-FOPID	0.35049	0.021662	1.0413	0.01702
MWOA-PIDn[43]	0.5251	0.0527	1.5033	0.0422
MWOA-PID[43]	0.4150	0.0258	1.9873	0.0200
BDGOA-PID	0.9215	0.0621	3.2569	0.1202
BDGOA-PI	1.2609	0.0882	7.4877	0.2002
RIME-PI[40]	0.8236	0.0559	3.0733	0.0994
BWOA-PI[44]	0.9979	0.0835	3.7909	0.1531
SSA-PI[45]	1.0240	0.0970	3.4662	0.1624
SFLA-PI[46]	3.2445	0.3903	23.7959	1.6722
FA-PI[34]	1.7207	0.2097	7.4259	0.4723
GA-PI[34]	2.3341	0.2802	12.1244	0.8616
GTO-PI[41]	0.8291	0.0578	3.0921	0.1010
WOA-PI[43]	1.3356	0.1235	5.2829	0.2860

Table 8. Comparison of the results for proposed and different controllers in scenario I.

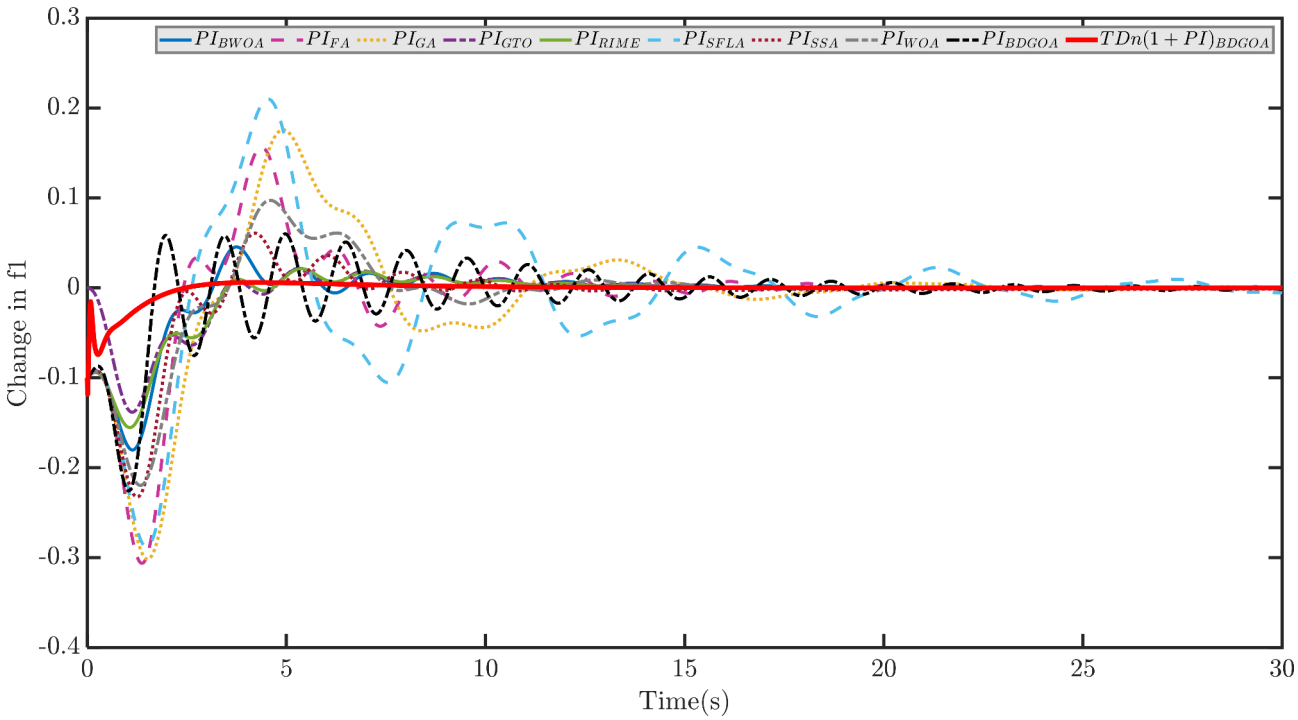


Fig. 14. Comparison of frequency variation Δf_1 for proposed and PI controllers in scenario II

stabilize the oscillations in the system. This highlights the controller's robustness and adaptability to changes in system parameters, ensuring reliable stability across different operating conditions.

Conclusions and scope of future work

In this work, we investigated the use of LFC in a two-area power system comprising a PV power plant and a reheat thermal generator. To address dynamic challenges such as frequency oscillations and tie-line power fluctuations, we developed an advanced multi-stage TDn(1 + PI) controller. The controller's parameters were optimized using the BDGOA, with an enhanced ITAE serving as the OF. The BDGOA-tuned TDn(1 + PI) controller was compared in detail to a number of other controllers, such as the BDGOA-tuned FOPID, MWOA-tuned PIDn, MWOA-tuned PID, BDGOA-tuned PID, BDGOA-tuned PI, RIME-tuned PI, BWOA-tuned PI, SSA-tuned PI, SFLA-tuned PI, FA-tuned PI, GA-tuned PI, GTO-tuned PI, and WOA-tuned PI controllers. Comprehensive simulation results consistently demonstrated that the BDGOA-tuned TDn(1 + PI) controller outperformed the alternatives, especially when it came to decreasing overshoot/undershoot values and attaining quicker system oscillation settling periods. Moreover, the proposed controller demonstrated excellent

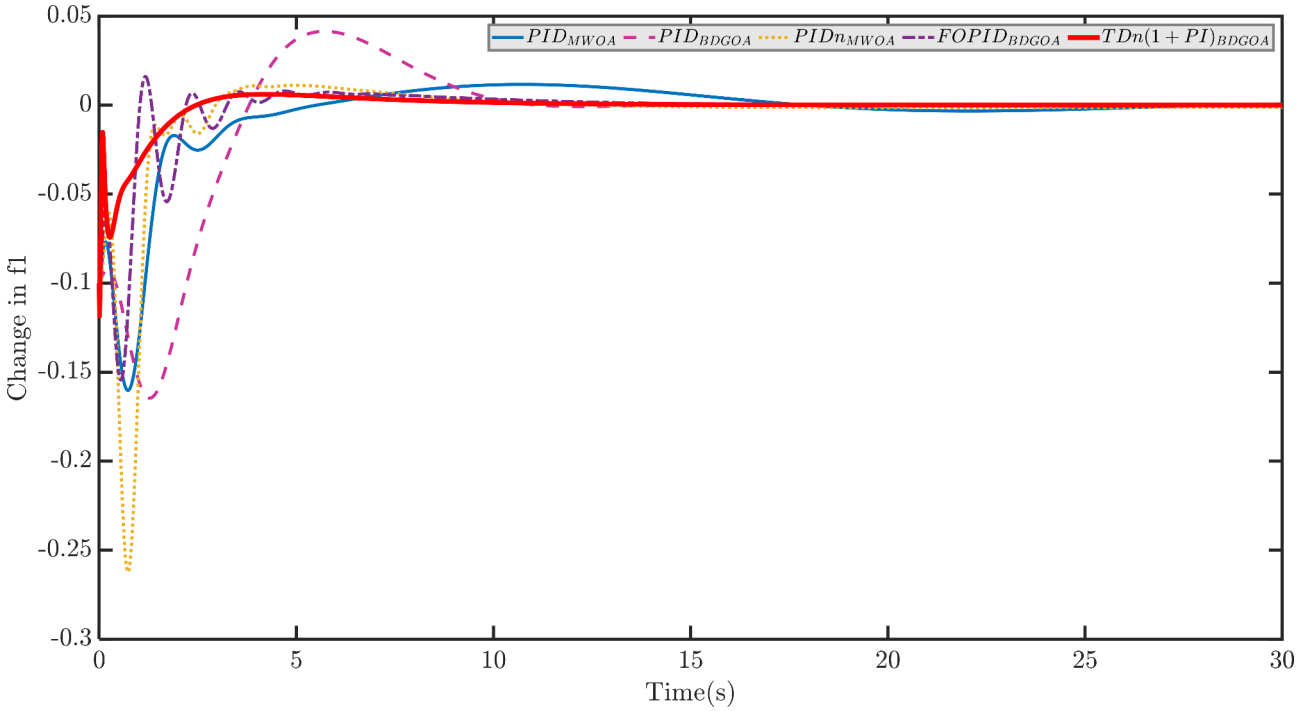


Fig. 15. Comparison of frequency variation Δf_1 for proposed and PID, PIDn and FOPID controllers in scenario II.

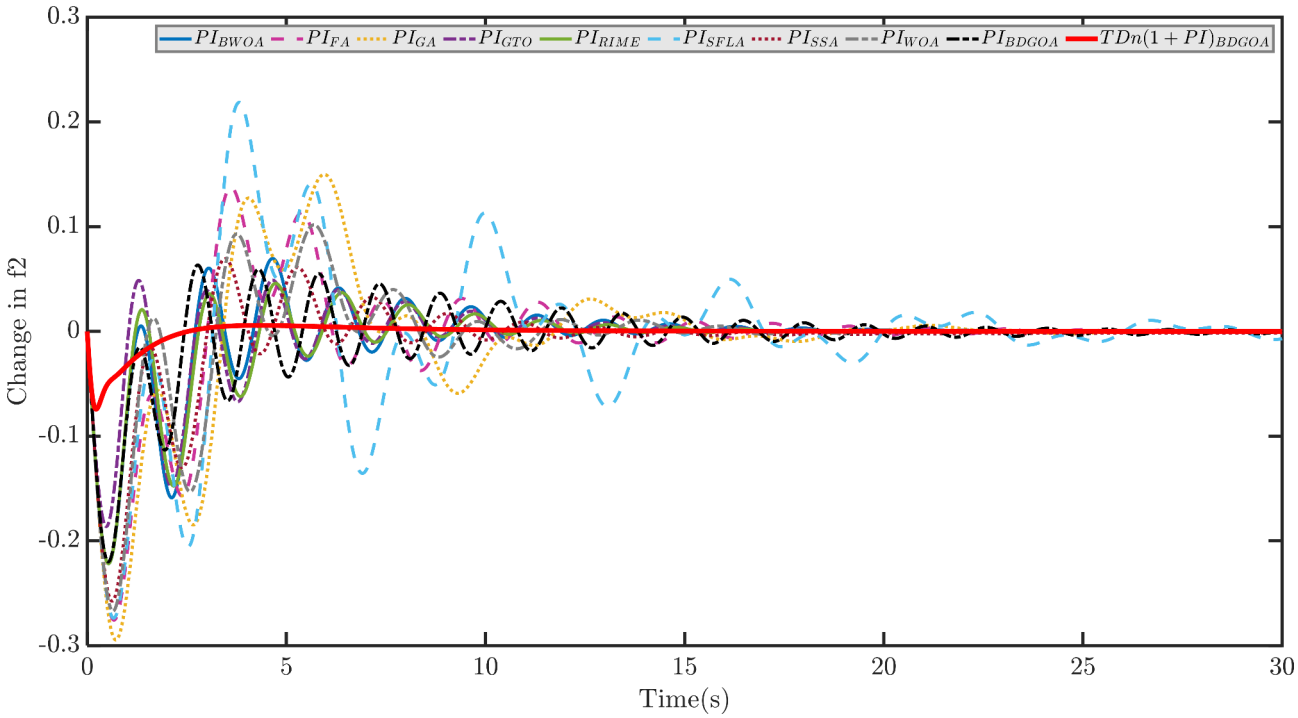


Fig. 16. Comparison of frequency variation Δf_2 for proposed and PI controllers in scenario II

performance under different operating conditions, such as random load changes, system parameter variations, stepwise load changes, and the presence of nonlinear factors. The robustness of the BDGOA-tuned TDn(1 + PI) controller was further validated through tests with parameter variations, where it maintained stable performance, confirming its reliability. These results lead us to the conclusion that the BDGOA-tuned TDn(1 + PI) controller dramatically increases power system stability and reliability and is a highly effective LFC solution in two-area

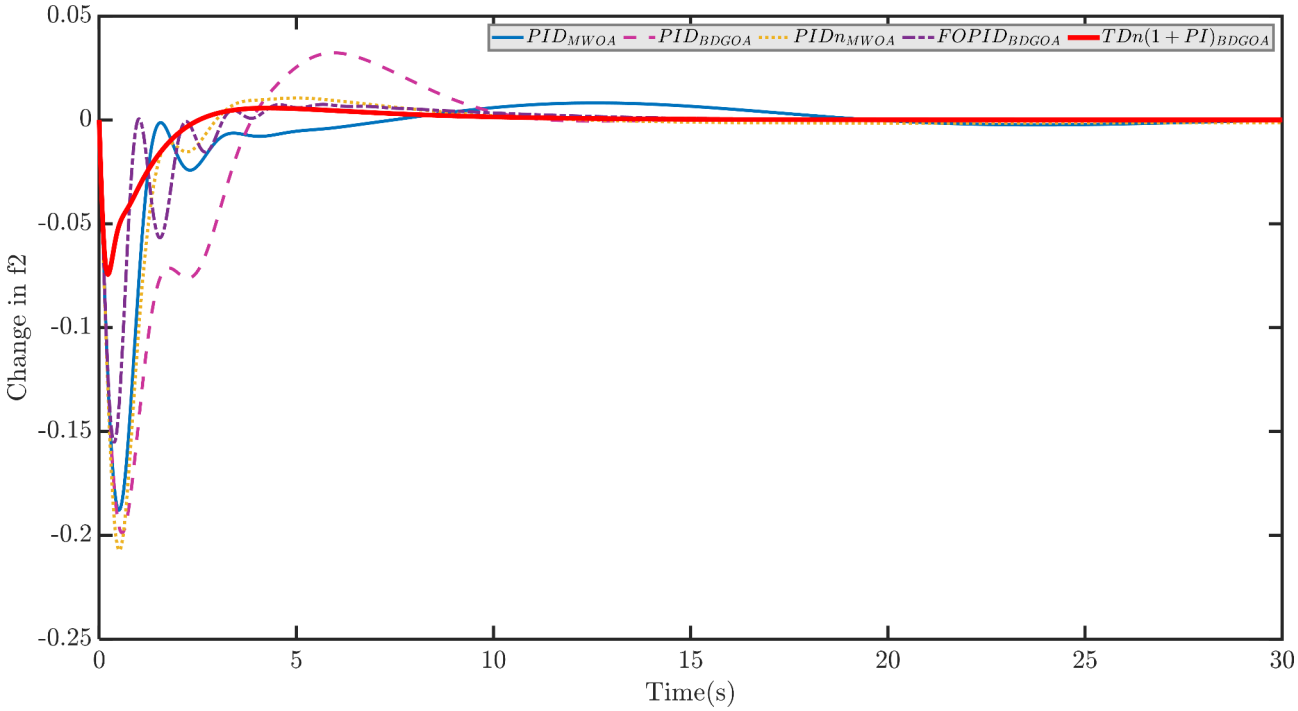


Fig. 17. Comparison of frequency variation Δf_2 for proposed and PID, PIDn and FOPID controllers in scenario II.

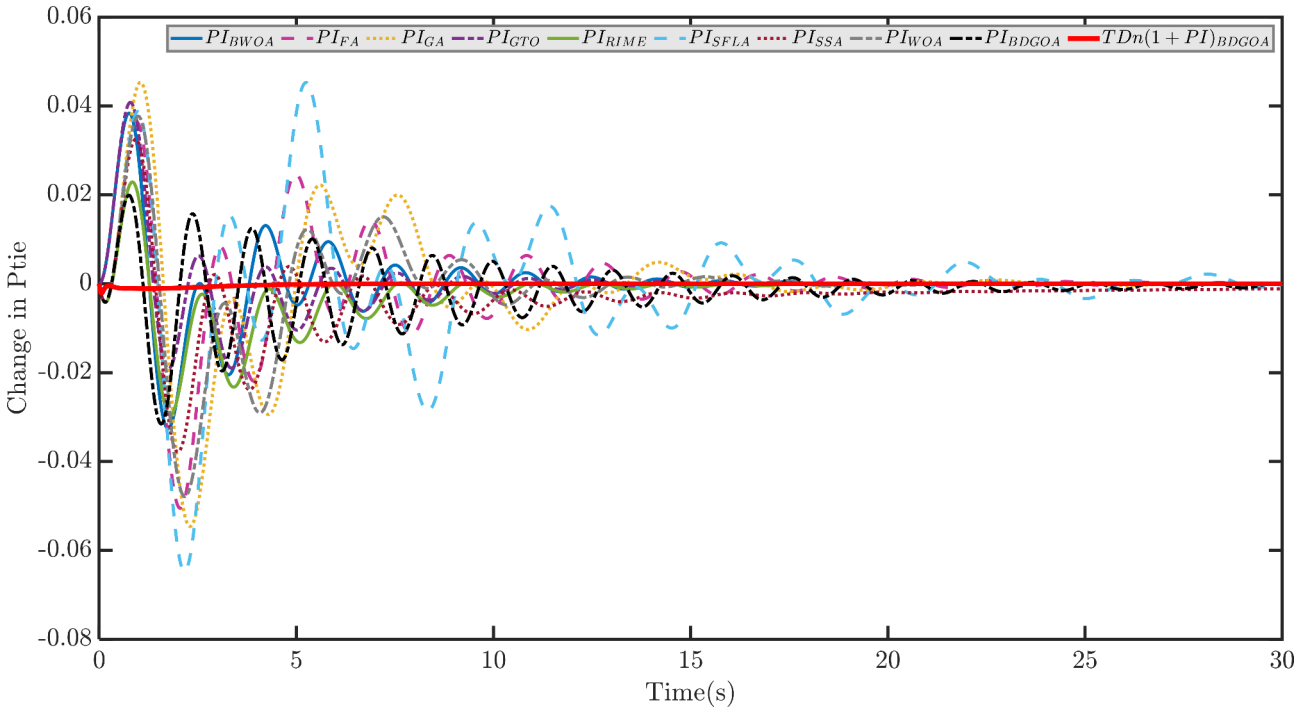


Fig. 18. Comparison of tie-line power deviation ΔP_{tie} for proposed and PI controllers in scenario II

PV-thermal systems. Additionally, this study highlights the critical role of LFC in ensuring operational efficiency and reliable energy supply in power systems. We recommend further empirical research using the OPAL-RT simulation platform and anticipate that ongoing development of optimization algorithms will lead to enhanced operational performance, particularly in LFC applications. The BDGOA-tuned TDn(1 + PI) controller emerges

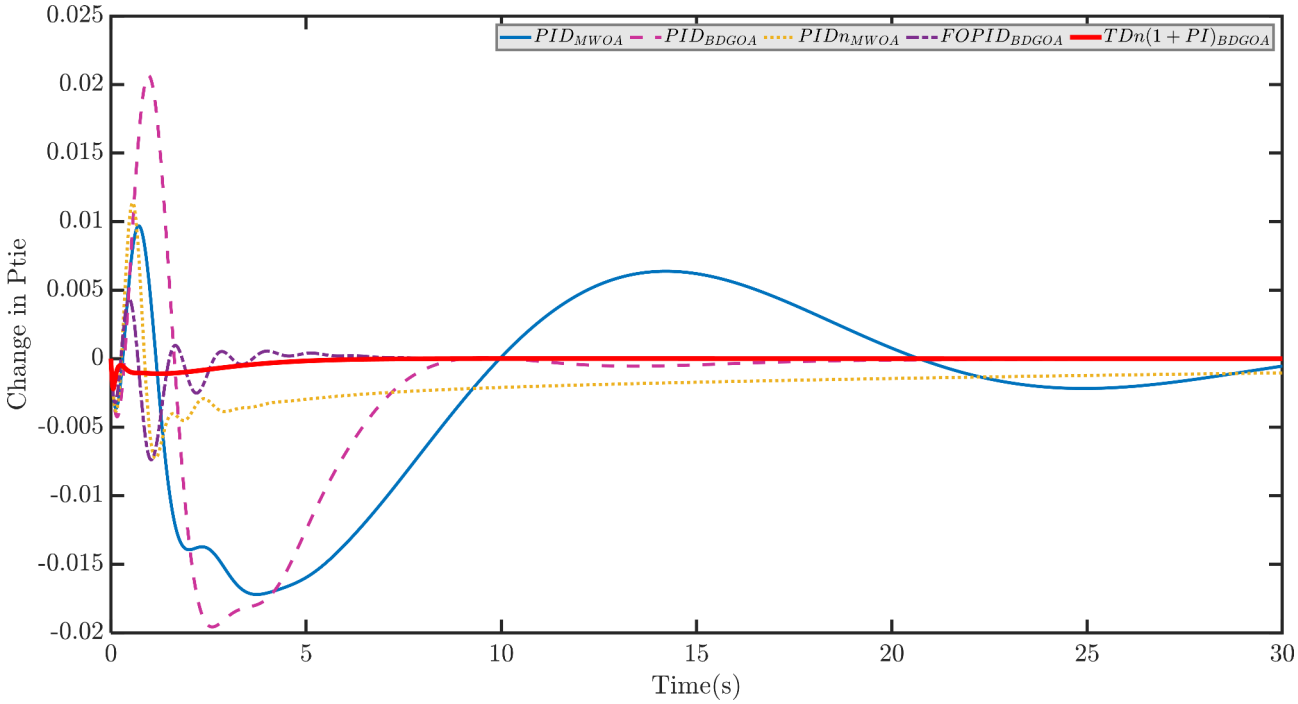


Fig. 19. Comparison of tie-line power deviation ΔP_{tie} for proposed and PID, PID*n* and FOPID controllers in scenario II.

Algorithm-Controller	Δf_1				Δf_2				ΔP_{tie}			
	ST (s)	US	OS	TP (s)	ST (s)	US	OS	TP (s)	ST (s)	US	OS	TP (s)
BDGOA-TD*n*(1 + PI) (Proposed)	0.026823	-0.11846	0.0060801	4.1918	0	-0.074418	0.005725	4.3008	0	-0.0022086	1.116e-05	11.2157
BDGOA-FOPID	0.77014	-0.15443	0.01608	1.1723	0.6161	-0.15517	0.0074841	50.0075	0	-0.0073828	0.0043535	0.47232
MWOA-PID*n*[43]	1.0812	-0.2623	0.0112	4.9300	1.0014	-0.2072	0.0106	5.0000	0	-0.0073	0.0114	0.5600
MWOA-PID[43]	1.1656	-0.1603	0.0116	10.7300	0.9281	-0.1879	0.0082	12.5800	0	-0.0172	0.0097	0.7100
BDGOA-PID	2.2208	-0.1646	0.0414	5.7190	1.2763	-0.1988	0.0323	5.9490	0	-0.0196	0.0206	0.9687
BDGOA-PI	1.4677	-0.2258	0.0601	4.9769	2.1030	-0.2200	0.0634	2.7822	1.7599	-0.0315	0.0199	0.7525
RIME-PI[40]	1.6219	-0.1553	0.0213	5.3726	2.4666	-0.2217	0.0459	4.7297	2.0045	-0.0296	0.0229	0.8463
BWOA-PI[44]	1.7001	-0.1802	0.0456	3.7444	2.4345	-0.2218	0.0696	4.6570	2.0241	-0.0338	0.0225	0.8233
SSA-PI[45]	1.9061	-0.2326	0.0608	4.2120	2.6423	-0.2575	0.0695	3.4658	2.3186	-0.0379	0.0325	0.9276
SFLA-PI[46]	5.2736	-0.2881	0.2101	4.5396	10.2835	-0.2738	0.2186	3.8152	8.5521	-0.0647	0.0453	5.2496
FA-PI[34]	4.8609	-0.3063	0.1565	4.3728	5.6082	-0.2757	0.1376	3.6128	2.5018	-0.0505	0.0364	0.9442
GA-PI[34]	5.9149	-0.3017	0.1759	4.9205	6.4615	-0.2946	0.1499	5.9553	4.5397	-0.0546	0.0453	1.0463
GTO-PI[41]	1.5515	-0.1382	0.0218	5.3192	2.4046	-0.1863	0.0489	4.6611	1.1134	-0.0191	0.0408	0.7920
WOA-PI[43]	2.1045	-0.2196	0.0974	4.5892	5.7760	-0.2671	0.1017	5.6949	4.3107	-0.0479	0.0377	0.9897

Table 9. Numerical results of ST, US, OS and TP for Δf_1, Δf_2, ΔP_{tie} in scenario II

as a promising tool for maintaining stable power system operation and reducing oscillations in similar hybrid power systems.

Algorithm-Controller	IAE	ISE	ITAE	ITSE
BDGOA-TDn(1 + PI) (Proposed)	0.20843	0.0066419	0.5601	0.0045789
BDGOA-FOPID	0.36292	0.024012	1.0254	0.017214
MWOA-PIDn[43]	0.6009	0.0602	2.6208	0.0463
MWOA-PID[43]	0.7529	0.0455	4.5959	0.1512
BDGOA-PID	1.0637	0.0923	3.2331	0.1202
BDGOA-PI	1.2867	0.0939	7.3984	0.1932
RIME-PI[40]	0.9051	0.0772	2.9150	0.1105
BWOA-PI[44]	0.9750	0.0864	3.5131	0.1318
SSA-PI[45]	1.1723	0.1222	4.9706	0.1766
SFLA-PI[46]	3.0593	0.3529	21.5626	1.3947
FA-PI[34]	1.7667	0.2215	7.3783	0.4635
GA-PI[34]	2.3784	0.3060	11.8846	0.8642
GTO-PI[41]	0.8291	0.0578	3.0921	0.1010
WOA-PI[43]	1.4271	0.1548	5.2619	0.3157

Table 10. Comparison of the results for proposed and different controllers in scenario II.

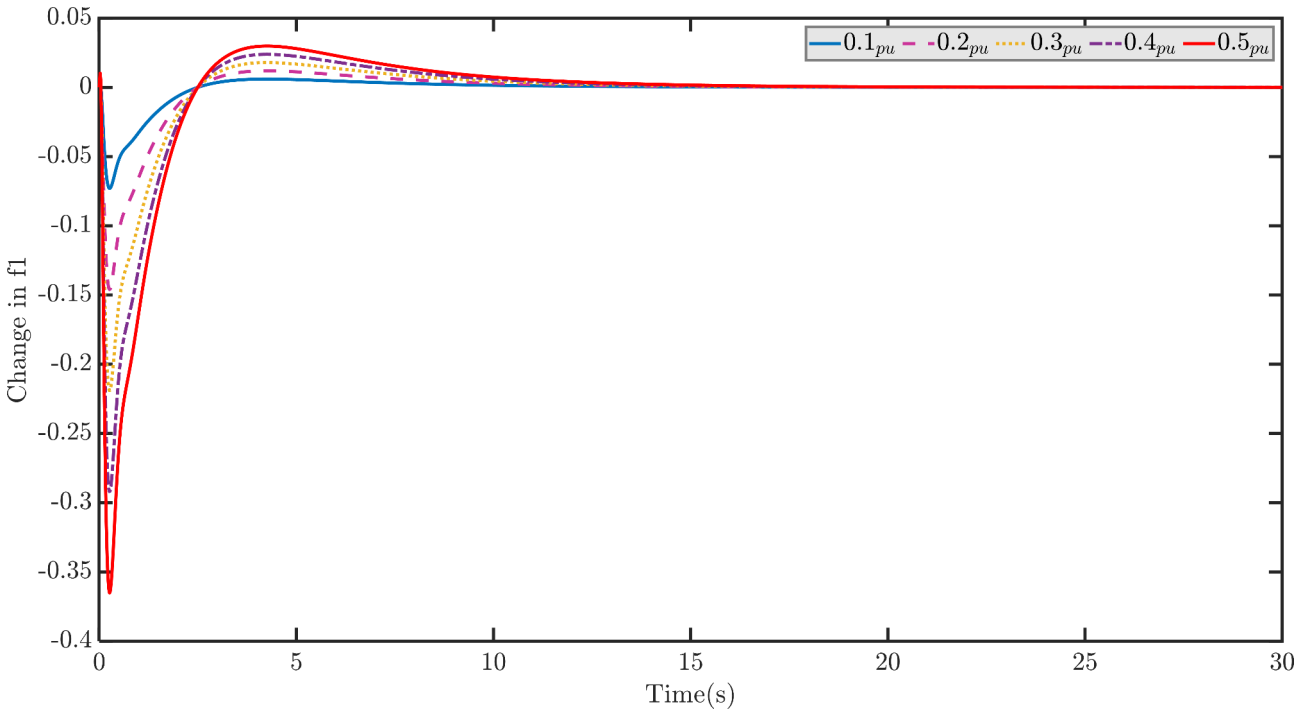


Fig. 20. Comparison of frequency variation Δf_1 for proposed controller in scenario III

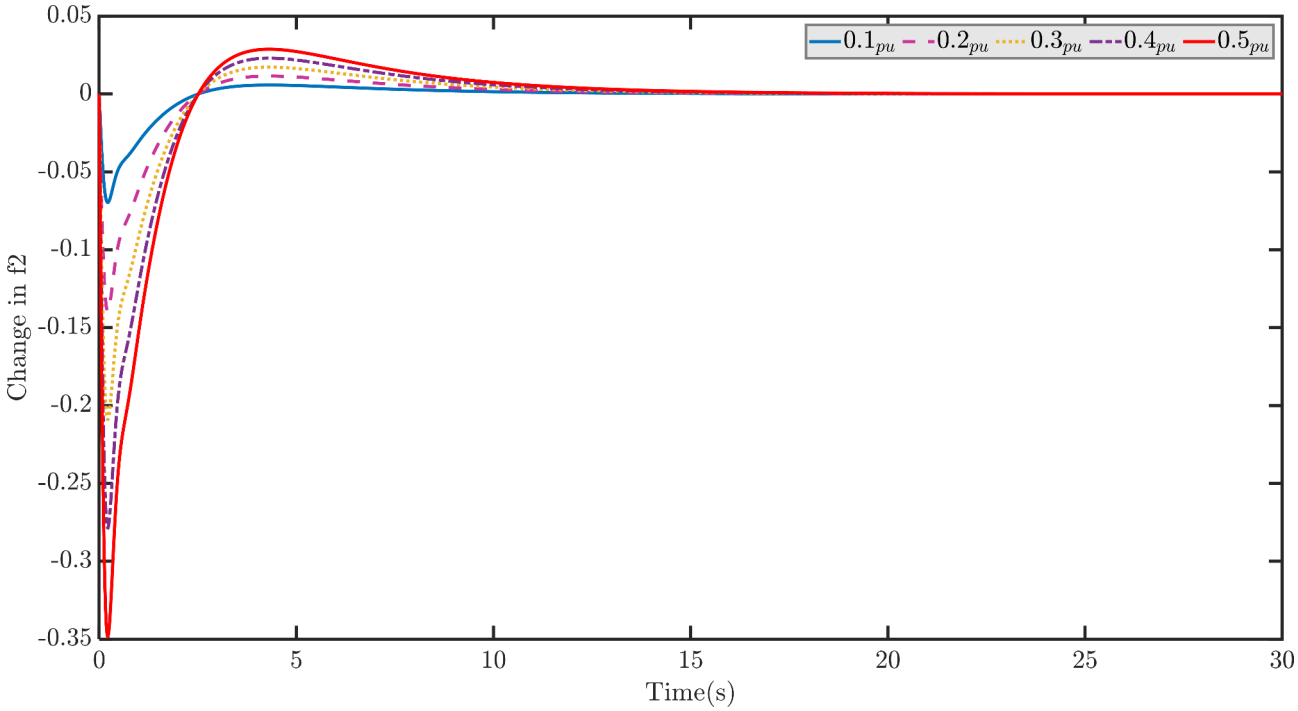


Fig. 21. Comparison of frequency variation Δf_2 for proposed controller in scenario III

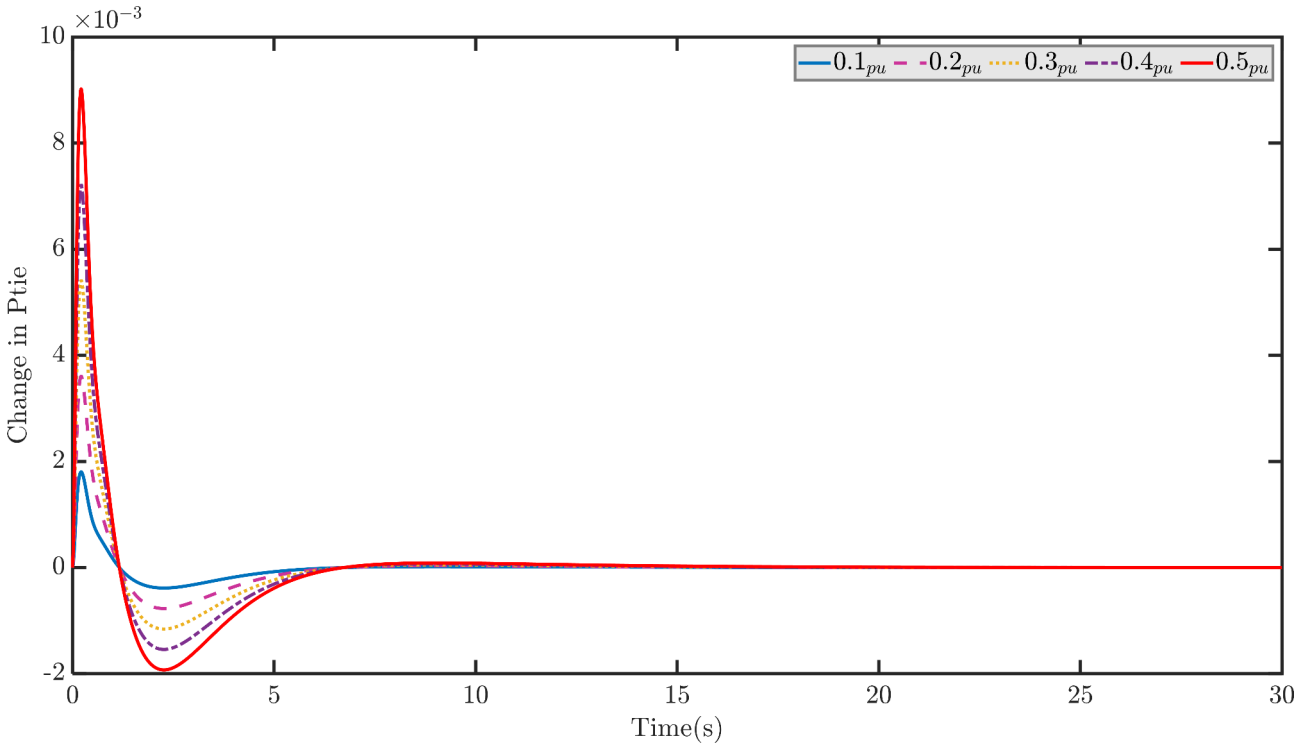


Fig. 22. Comparison of tie-line power deviation ΔP_{tie} for proposed controller in scenario III

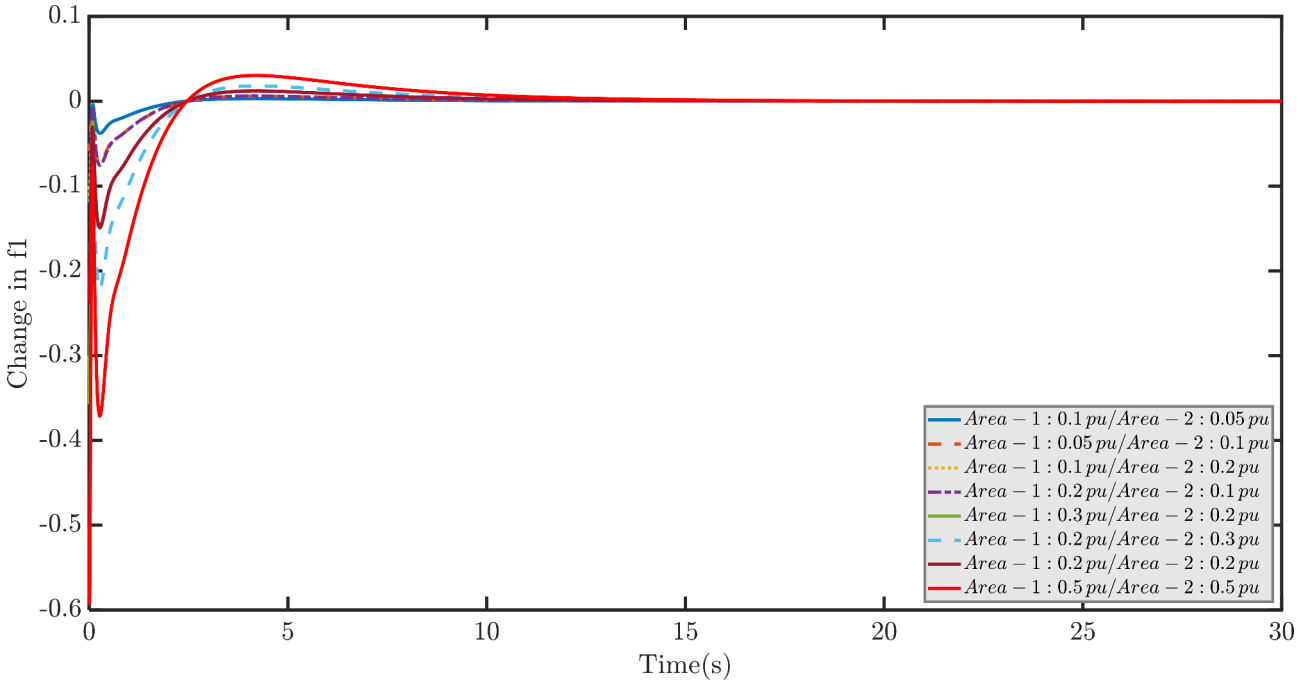


Fig. 23. Comparison of frequency variation Δf_1 for proposed controller in scenario IV

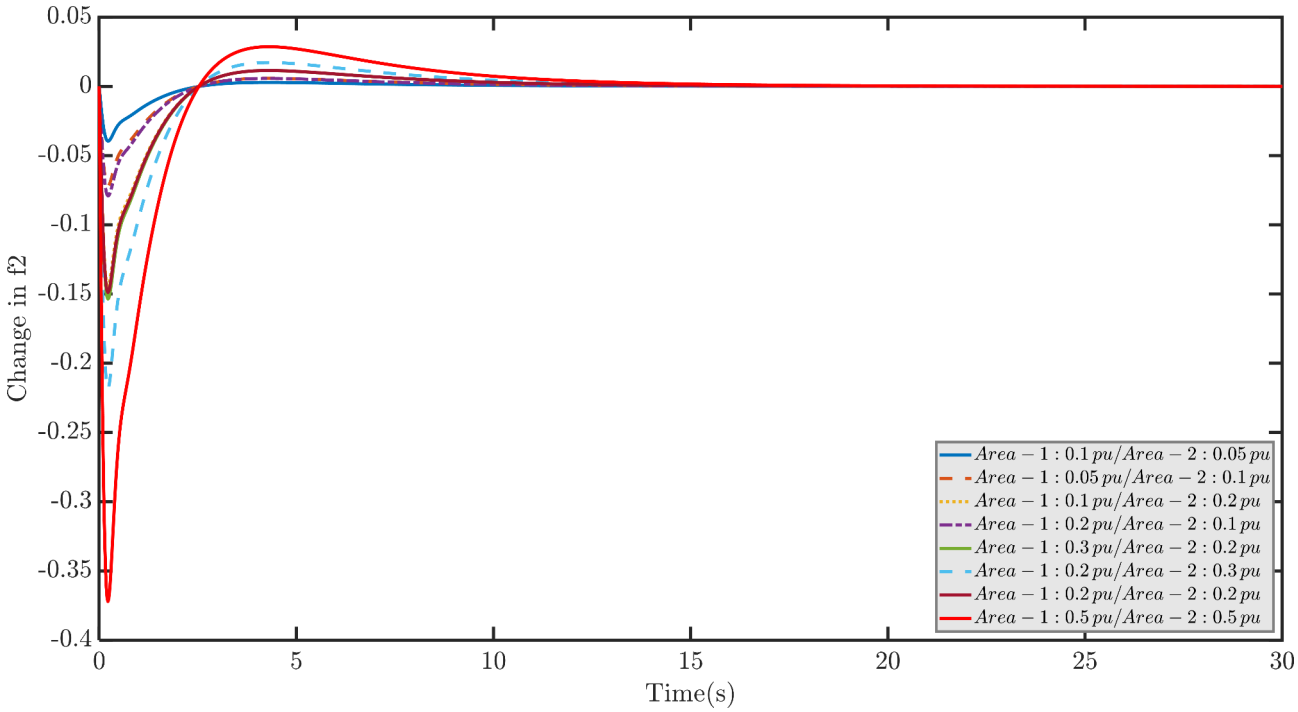


Fig. 24. Comparison of frequency variation Δf_2 for proposed controller in scenario IV

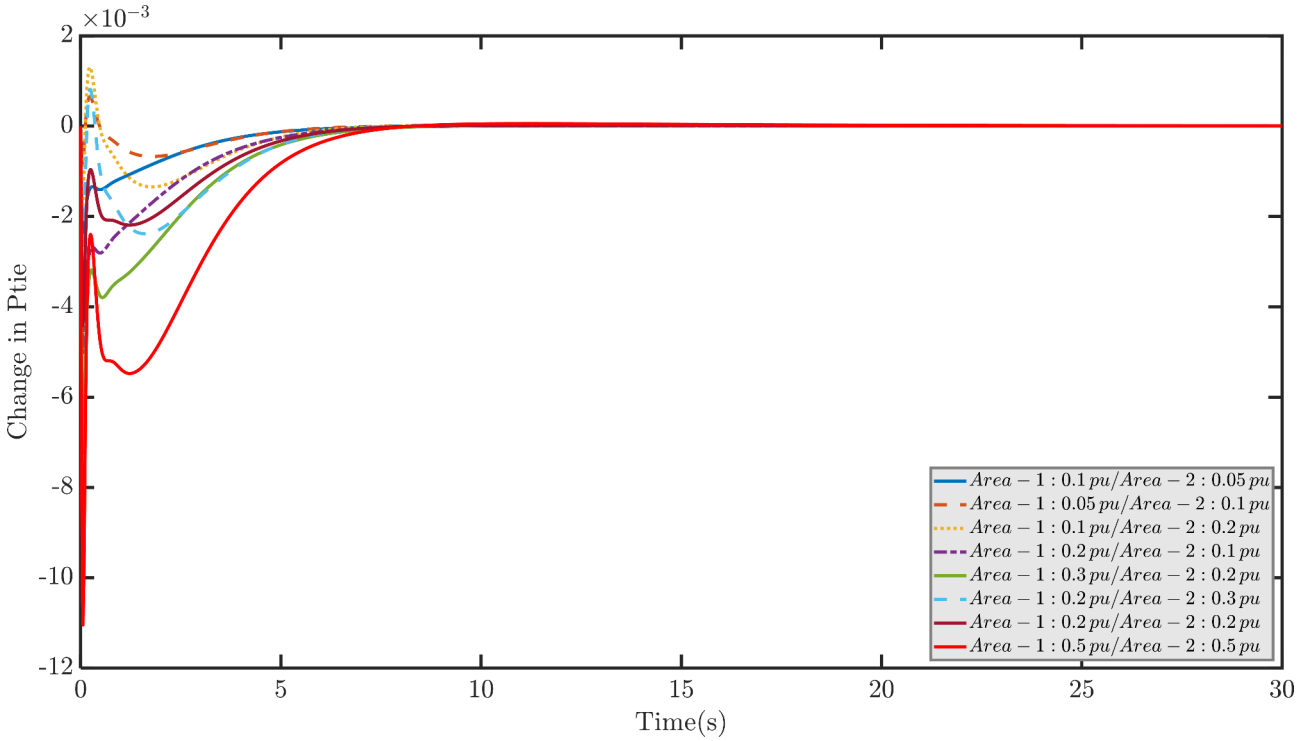


Fig. 25. Comparison of tie-line power deviation ΔP_{tie} for proposed controller in scenario IV

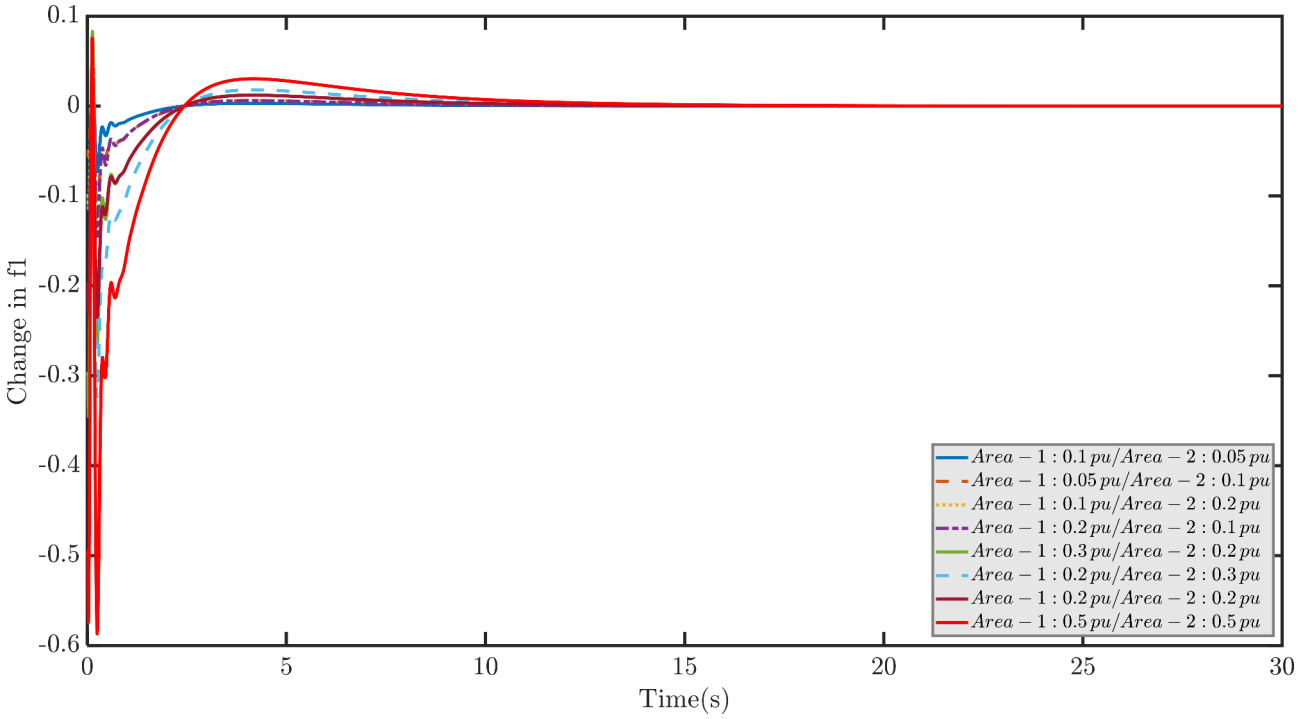


Fig. 26. Comparison of frequency variation Δf_1 for proposed controller in scenario V

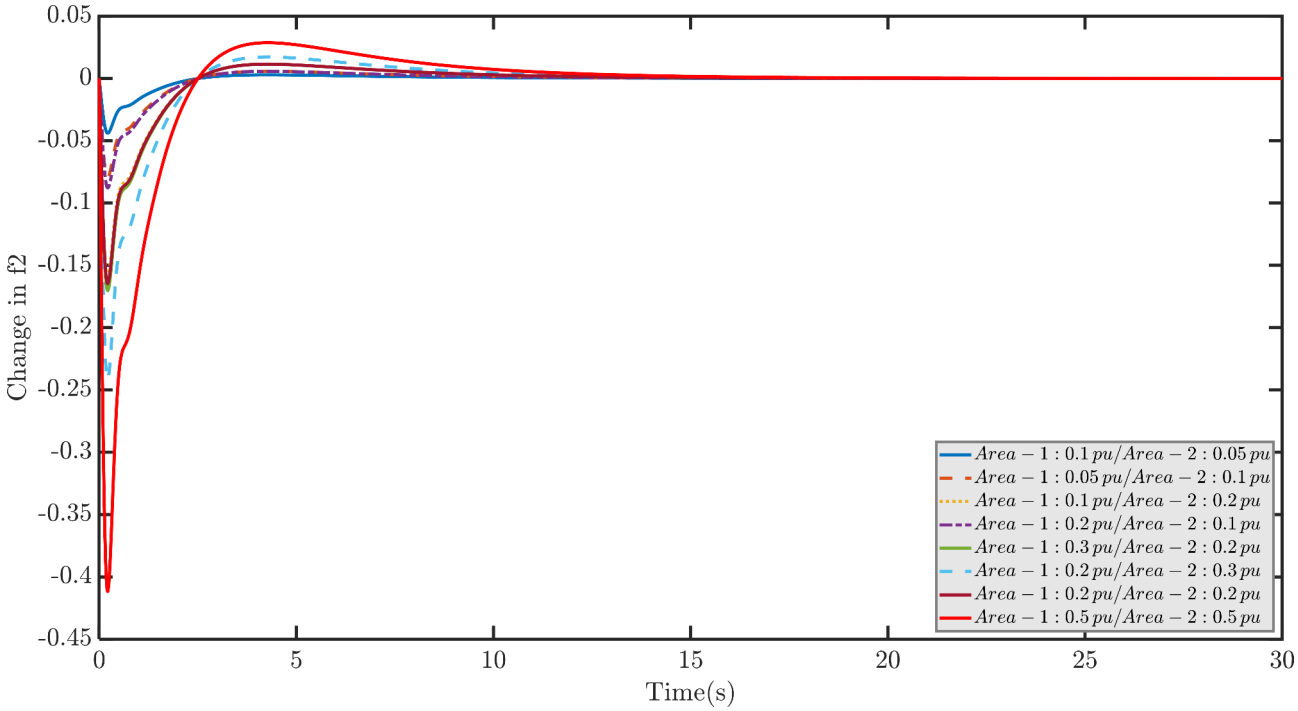


Fig. 27. Comparison of frequency variation Δf_2 for proposed controller in scenario V

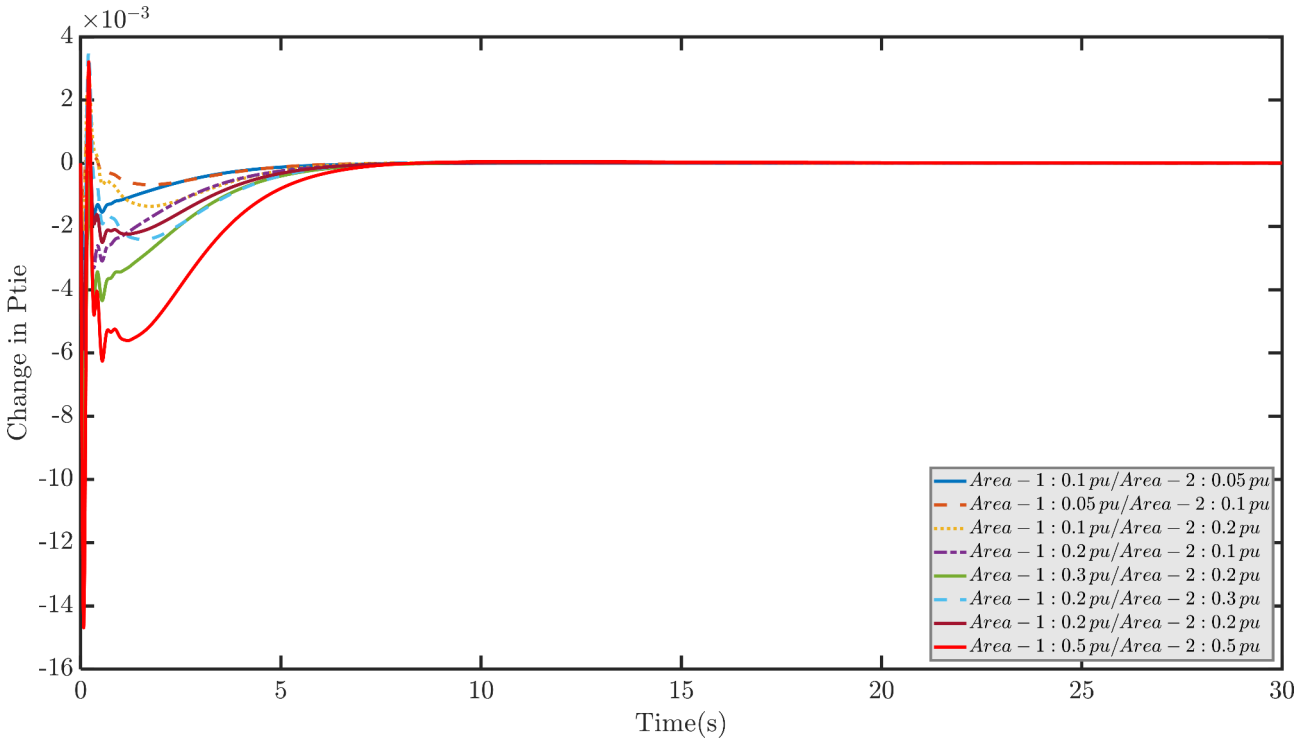


Fig. 28. Comparison of tie-line power deviation ΔP_{tie} for proposed controller in scenario V

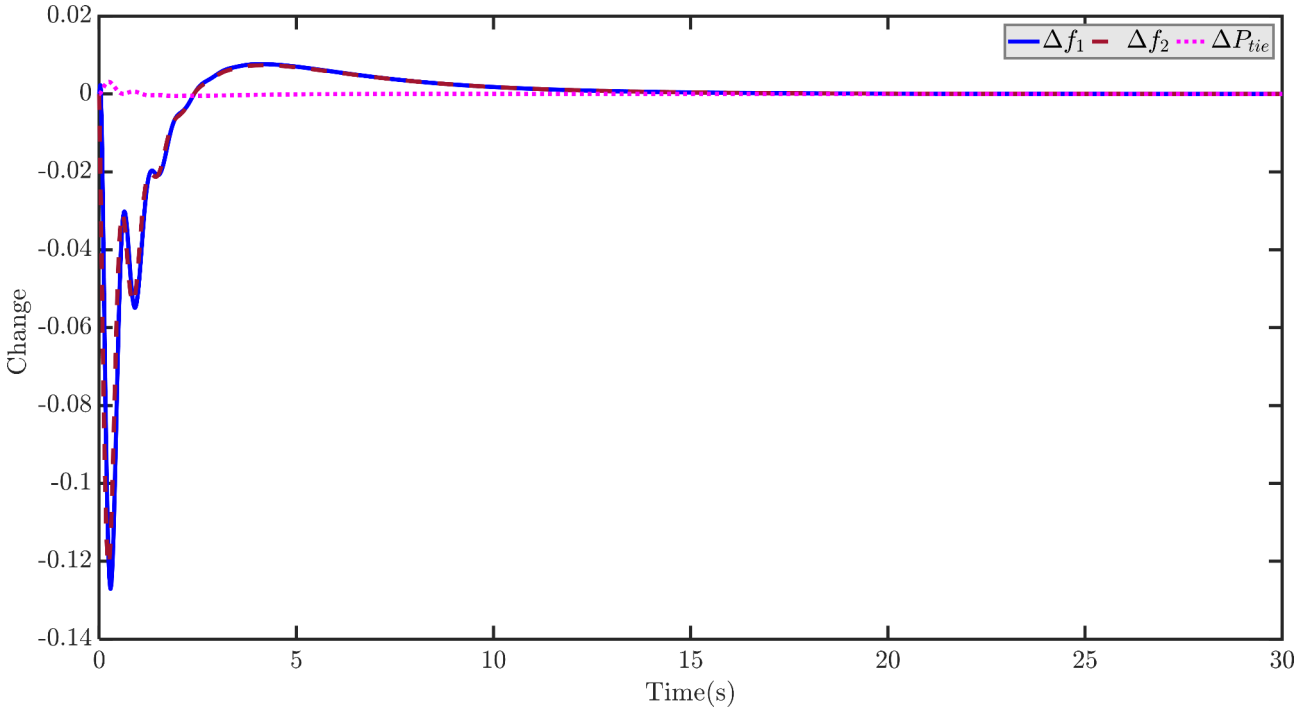


Fig. 29. Comparison of variation Δf_1, Δf_2 and ΔP_{tie} for proposed controller with GDB in scenario VI

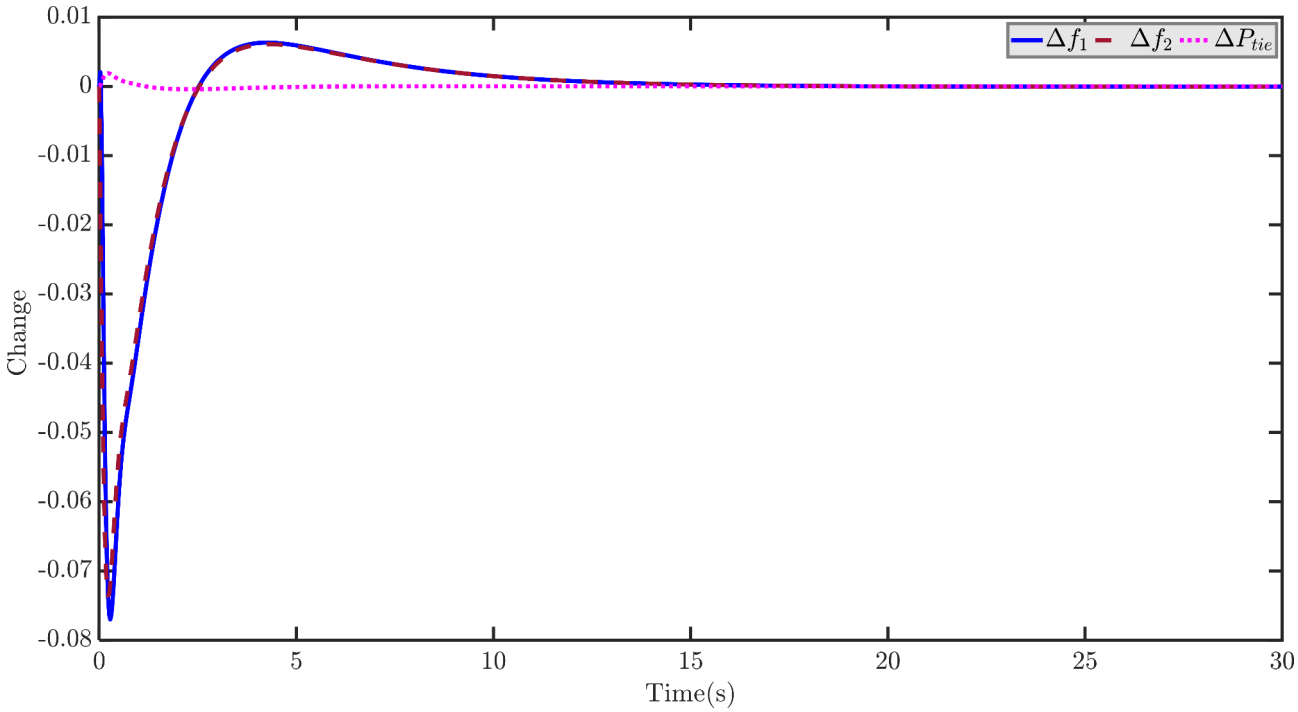


Fig. 30. Comparison of variation Δf_1, Δf_2 and ΔP_{tie} for proposed controller with BD in scenario VI

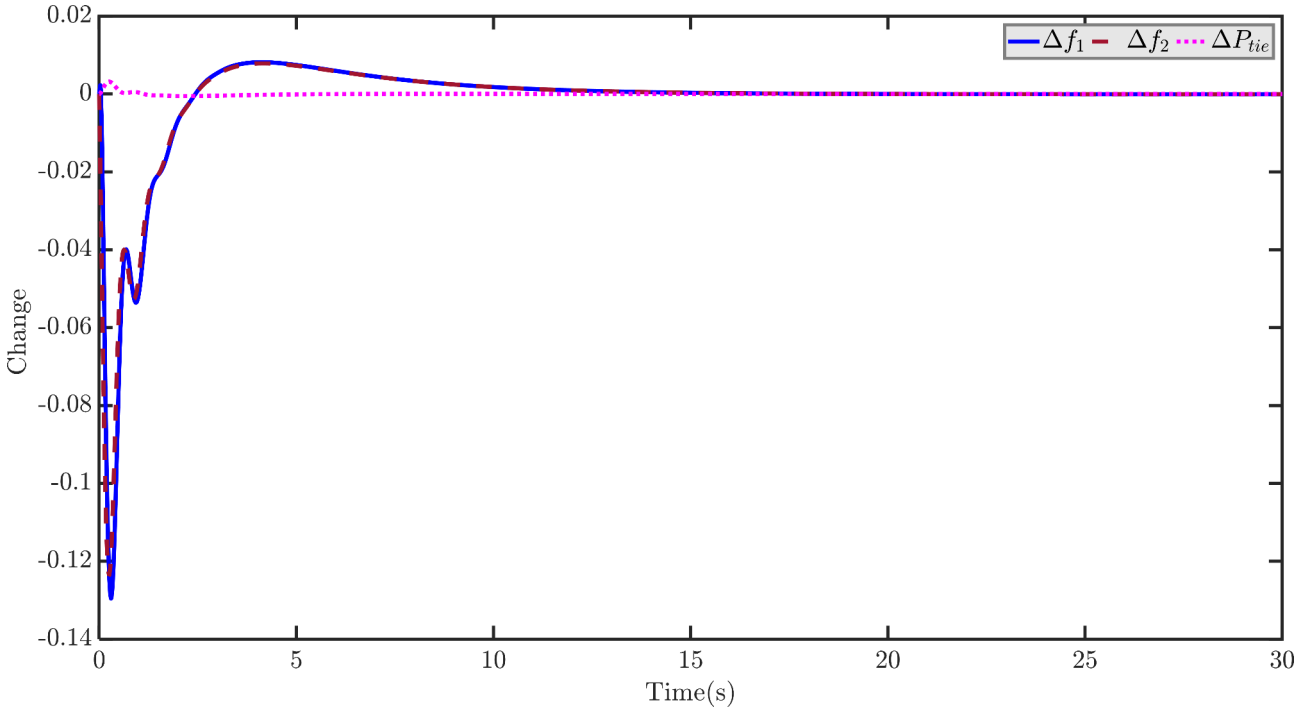


Fig. 31. Comparison of variation Δf_1 , Δf_2 and ΔP_{tie} for proposed controller with GDB and BD in scenario VI

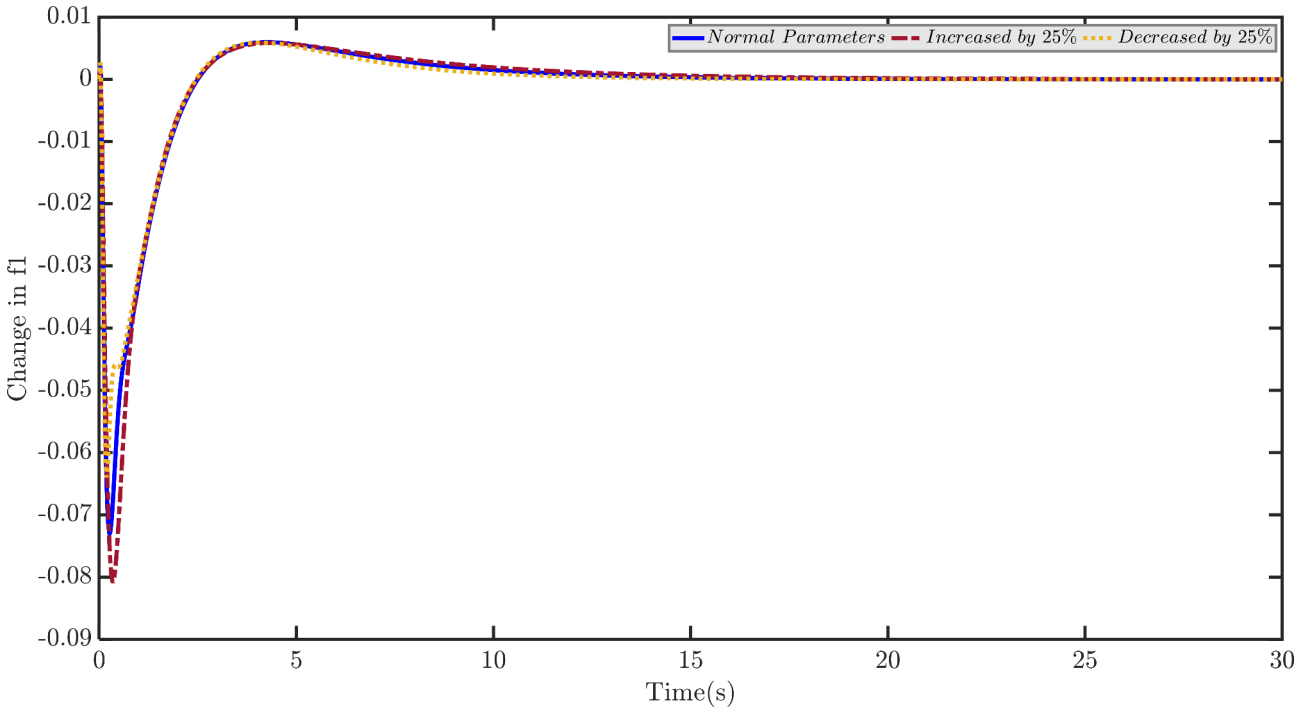


Fig. 32. Comparison of frequency variation Δf_1 for proposed controller in scenario VII

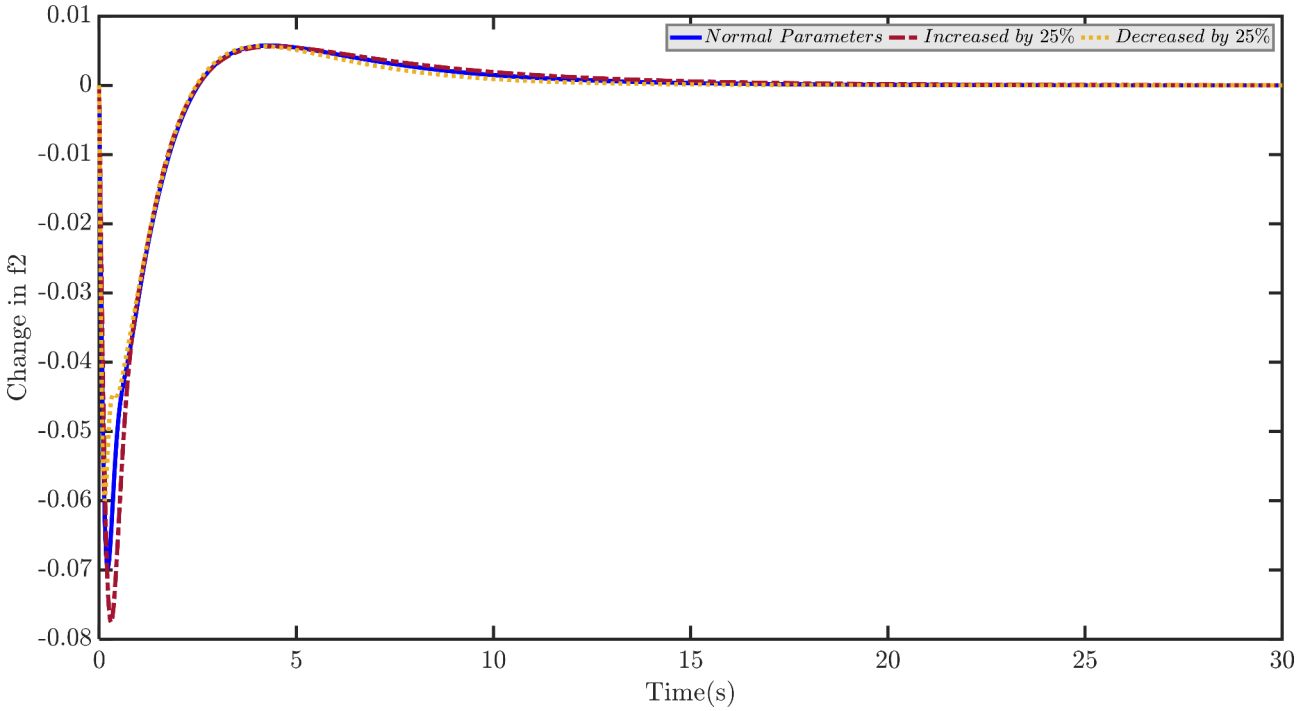


Fig. 33. Comparison of frequency variation Δf_2 for proposed controller in scenario VII

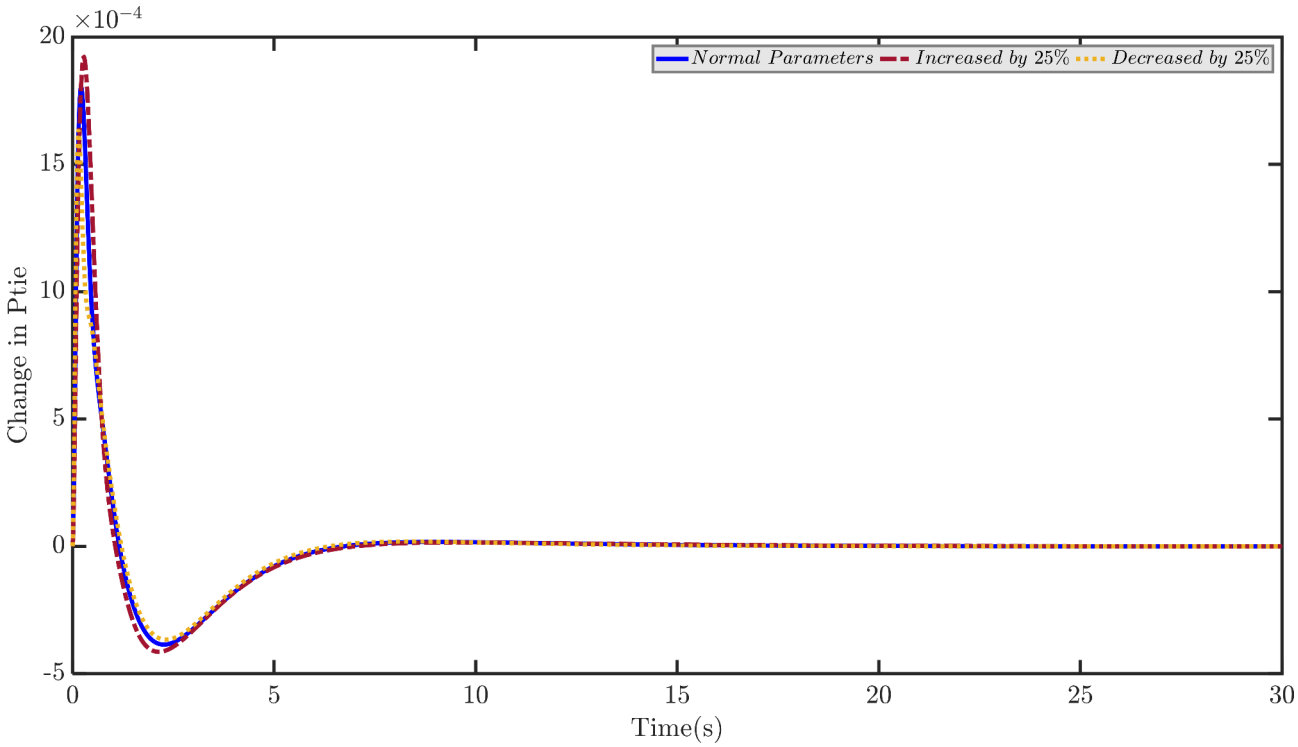


Fig. 34. Comparison of tie-line power deviation ΔP_{tie} for proposed controller in scenario VII

Data availability

The datasets used and/or analyzed during the current study available from the corresponding author on reasonable request.

Received: 13 October 2024; Accepted: 26 November 2024

Published online: 28 November 2024

References

1. Ranjan, M. & Shankar, R. A literature survey on load frequency control considering renewable energy integration in power system: recent trends and future prospects. *J. Energy Storage*. **45**, 103717 (2022).
2. Gulzar, M. M. et al. Load frequency control (LFC) strategies in renewable energy-based Hybrid Power systems: a review. *Energies (Basel)*. **15**, 3488 (2022).
3. Arya, Y. Automatic generation control of two-area electrical power systems via optimal fuzzy classical controller. *J. Frankl. Inst.* **355**, 2662–2688 (2018).
4. Sattar, F. et al. A predictive tool for power system operators to ensure frequency stability for power grids with renewable energy integration. *Appl. Energy*. **353**, 122226 (2024).
5. Sun, B. et al. An Energy Storage Capacity Configuration Method for a Provincial Power System considering Flexible Adjustment of the Tie-Line. *Energies (Basel)*. **17**, 270 (2024).
6. Dunna, V. K. et al. Super-twisting MPPT control for grid-connected PV/battery system using higher order sliding mode observer. *Sci. Rep.* **14** (1), 16597 (2024).
7. Izci, D., Abualigah, L., Can, Ö., Andiç, C. & Ekinci, S. Achieving improved stability for automatic voltage regulation with fractional-order PID plus double-derivative controller and mountain gazelle optimizer. *Int. J. Dynamics Control.* **1**, 1–6 (2024 Feb).
8. Aribowo, W., Abualigah, L., Oliva, D. & Prapanca, A. A novel modified mountain gazelle optimizer for tuning parameter proportional integral derivative of DC motor. *Bull. Electr. Eng. Inf.* **13** (2), 745–752 (2024).
9. Widi Aribowo, R. et al. Controlling parameters proportional integral derivative of DC motor using a gradient-based optimizer. *Int. J. Power Electron. Drive Syst. (IJPEDS)Vol.* **15** (2), 696– (June 2024).
10. Premkumar, M. et al. Optimal operation and control of hybrid power systems with stochastic renewables and FACTS devices: an intelligent multi-objective optimization approach. *Alexandria Eng. J.* **93**, 90–113 (2024).
11. Pandya, S. B. et al. Multi-objective RIME algorithm-based techno economic analysis for security constraints load dispatch and power flow including uncertainties model of hybrid power systems. *Energy Rep.* **11**, 4423–4451 (2024).
12. Alsmadi, O., Abu-Hammour, Z. & Mahafzah, K. Digital systems model order reduction with substructure preservation and fuzzy logic control. *Eurasia Proc. Sci. Technol. Eng. Math.* **28**, 14–22 (2024).
13. Abualigah, L., Ekinci, S. & Izci, D. Aircraft Pitch Control via filtered proportional-integral-derivative Controller Design using Sinh Cosh Optimizer. *Int. J. Rob. Control Syst.* **4** (2), 746–757 (2024).
14. Alrashed, M. M., Flah, A., Dashtdar, M., El-Bayeh, C. Z. & Elnaggar, M. F. Improving the control strategy of the DVR Compensator based on an adaptive notch filter with an optimized PD Controller using the IGWO Algorithm. *Int. Trans. Electr. Energy Syst.* **2024** (1), 5097056 (2024).
15. Fadheel, B. A. et al. A Hybrid Sparrow Search Optimized Fractional Virtual Inertia Control for Frequency Regulation of Multi-Microgrid System. *IEEE Access*. Mar 18. (2024).
16. Abualigah, L., Izci, D., Ekinci, S. & Zitar, R. A. Optimizing aircraft Pitch Control systems: a Novel Approach integrating Artificial rabbits optimizer with PID-F Controller. *Int. J. Rob. Control Syst.* **4** (1), 354–364 (2024).
17. Izci, D. et al. Refined Sinh cosh optimizer tuned controller design for enhanced stability of automatic voltage regulation. *Electr. Eng.* **29**, 1–4 (2024 Mar).
18. Izci, D. et al. A novel control scheme for automatic voltage regulator using novel modified artificial rabbits optimizer. *E-Prime-Advances Electr. Eng. Electron. Energy*. **6**, 100325 (2023).
19. Altawil, I. et al. Optimization of fractional order PI controller to regulate grid voltage connected photovoltaic system based on slap swarm algorithm. *Int. J. Power Electron. Drive Syst. (IJPEDS)*. **14**, 1184–1200 (2023).
20. Abualigah, L., Ekinci, S., Izci, D. & Zitar, R. A. Modified Elite Opposition-based Artificial Hummingbird Algorithm for Designing FOPID Controlled Cruise Control System. *Intell. Autom. Soft Comput.* ;**38**(2). (2023).
21. Sarayrah, A., Haj-ahmed, M. A. & Feilat, E. A. A Study of a Damping Control Based Predictive Strategy on an Inter-Area Power System. *In IEEE PES GTD International Conference and Exposition (GTD)* 2023 May 22 (pp. 60–66). IEEE. (2023).
22. Arya, Y. AGC of two-area electric power systems using optimized fuzzy PID with filter plus double integral controller. *J. Frankl. Inst.* **355**, 4583–4617 (2018).
23. Ni, L., Li, Y., Zhang, L. & Wang, G. A modified aquila optimizer with wide plant adaptability for the tuning of optimal fractional proportional–integral–derivative controller. *Soft Comput.* **28**, 6269–6305 (2024).
24. Sagor, A. R. et al. Pelican optimization algorithm-based proportional–integral–derivative Controller for Superior frequency regulation in interconnected Multi-area Power Generating System. *Energies (Basel)*. **17**, 3308 (2024).
25. Gulzar, M. M., Sibtain, D. & Khalid, M. Innovative design for enhancing transient stability with an ATFOPID controller in hybrid power systems. *J. Energy Storage*. **99**, 113364 (2024).
26. Qu, Z. et al. Optimized PID Controller for load frequency control in multi-source and Dual-Area Power Systems Using PSO and GA algorithms. *IEEE Access.* 1–1. https://doi.org/10.1109/ACCESS.2024.3445165 (2024).
27. Mishra, A. K., Sharma, P., Siguerdidjane, H., Mishra, P. & Mathur, H. D. Maiden Application of Integral-Tilt Integral Derivative with Filter (I-TDN) Control structure for load frequency control. *IFAC-PapersOnLine* **55**, 72–77 (2022).
28. Arya, Y. AGC of PV-thermal and hydro-thermal power systems using CES and a new multi-stage FPIDF-(1 + PI) controller. *Renew. Energy*. **134**, 796–806 (2019).
29. Shayeghi, H. & Rahnama, A. Designing a PD-(1 + PI) controller for LFC of an entirely renewable microgrid using PSO-TVAC. *Int. J. Techni Physi Prob Eng. (IJTPE)*. **12**, 19–27 (2020).
30. Parvin, K. et al. Intelligent Controllers and Optimization Algorithms for Building Energy Management towards Achieving Sustainable Development: challenges and prospects. *IEEE Access.* **9**, 41577–41602 (2021).
31. Jabari, M. & Rad, A. Optimization of Speed Control and Reduction of Torque Ripple in switched Reluctance motors using Metaheuristic algorithms based PID and FOPID controllers at the Edge. *Tsinghua Sci. Technol.* https://doi.org/10.26599/TST.2024.9010021 (2024).
32. Deng, W., Xu, J. & Zhao, H. An Improved ant colony optimization Algorithm based on hybrid strategies for Scheduling Problem. *IEEE Access.* **7**, 20281–20292 (2019).
33. Milani, A. E. & Mozafari, B. Genetic algorithm based optimal load frequency control in two-area interconected power systems. *Glob J. Technol. Optim.* **2**, 6–10 (2011).
34. Abd-Elazim, S. M. & Ali, E. S. Load frequency controller design of a two-area system composing of PV grid and thermal generator via firefly algorithm. *Neural Comput. Appl.* **30**, 607–616 (2018).
35. Sharma, M., Prakash, S., Saxena, S. & Dhundhara, S. Optimal fractional-Order Tilted-Integral-Derivative Controller for frequency stabilization in Hybrid Power System using salp swarm algorithm. *Electr. Power Compon. Syst.* **48**, 1912–1931 (2020).
36. Mohanty, D. & Panda, S. Modified salp swarm algorithm-optimized fractional-order adaptive fuzzy PID Controller for frequency regulation of Hybrid Power System with Electric Vehicle. *J. Control Autom. Electr. Syst.* **32**, 416–438 (2021).
37. Mishra, D., Nayak, P. C., Bhoi, S. K. & Prusty, R. C. Design and analysis of Multi-stage TDF/(1 + TI) controller for Load-frequency control of A.C Multi-Islanded Microgrid system using Modified Sine cosine algorithm. in *1st Odisha International Conference on Electrical Power Engineering, Communication and Computing Technology(ODICON)* 1–6 (IEEE, 2021). doi: (2021). https://doi.org/10.1109/ODICON50556.2021.9428969

38. Shayeghi, H. & Rahnama, A. Frequency regulation of a standalone interconnected AC Microgrid using innovative multistage TDF(1 + FOPI) Controller. *J. Operation Autom. Power Eng.* **12**, 121–133 (2024).
39. Shayeghi, H., Rahnama, A. & Bizon, N. TFODn-FOPI multi-stage controller design to maintain an islanded microgrid load-frequency balance considering responsive loads support. *IET Generation Transmission Distribution*. **17**, 3266–3285 (2023).
40. Ekinci, S. et al. Automatic Generation Control of a hybrid PV-Reheat Thermal Power System using RIME algorithm. *IEEE Access.* **12**, 26919–26930 (2024).
41. Can, O. & Ayas, M. S. Gorilla troops optimization-based load frequency control in PV-thermal power system. *Neural Comput. Appl.* **36**, 4179–4193 (2024).
42. Gomaa Haroun, A. H. & Li, Y. A novel optimized hybrid fuzzy logic intelligent PID controller for an interconnected multi-area power system with physical constraints and boiler dynamics. *ISA Trans.* **71**, 364–379 (2017).
43. Khadanga, R. K., Kumar, A. & Panda, S. A novel modified whale optimization algorithm for load frequency controller design of a two-area power system composing of PV grid and thermal generator. *Neural Comput. Appl.* **32**, 8205–8216 (2020).
44. Dahiya, P. & Saha, A. K. Frequency regulation of Interconnected Power System Using Black Widow Optimization. *IEEE Access.* **10**, 25219–25236 (2022).
45. Çelik, E., Öztürk, N. & Houssein, E. H. Influence of energy storage device on load frequency control of an interconnected dual-area thermal and solar photovoltaic power system. *Neural Comput. Appl.* **34**, 20083–20099 (2022).
46. Khadanga, R. K., Kumar, A. & Panda, S. A hybrid shuffled frog-leaping and pattern search algorithm for load frequency controller design of a two-area system composing of PV grid and thermal generator. *Int. J. Numer. Model. Electron. Networks Devices Fields* **33**, (2020).
47. Khadanga, R. K. & Kumar, A. Hybrid adaptive 'gbest'-guided gravitational search and pattern search algorithm for automatic generation control of multi-area power system. *IET Generation Transmission Distribution*. **11**, 3257–3267 (2017).
48. Tomy, F. T. & Prakash, R. Load frequency control of a two area hybrid system consisting of a grid connected PV system and thermal generator. *IJRET: Int. J. Res. Eng. Technol.* **3**, 573–580 (2014).
49. Rizk-Allah, R. M., Snášel, V., Izci, D. & Ekinci, S. Spiral-refraction mutation prairie dog algorithm: optimization framework for engineering design of interconnected multimachine power system. *Appl. Soft Comput.* **165**, 112036 (2024).
50. Rizk-Allah, R. M. et al. Incorporating adaptive local search and experience-based perturbed learning into artificial rabbits optimizer for improved DC motor speed regulation. *Int. J. Electr. Power Energy Syst.* **162**, 110266 (2024).
51. Izci, D. et al. Dynamic load frequency control in power systems using a hybrid simulated annealing based quadratic interpolation optimizer. *Sci. Rep.* **14**, 26011 (2024).

Acknowledgements

This article has been produced with the financial support of the European Union under the REFRESH – Research Excellence For Region Sustainability and High-tech Industries project number CZ.10.03.01/00/22_003/0000048 via the Operational Programme Just Transition and paper was supported by the following project TN02000025 National Centre for Energy II. The authors would like to express their sincere gratitude to Stanislav Misak for his exceptional supervision, project administration, and overall guidance throughout the course of this project. His expertise and support were instrumental to its success.

Author contributions

Mostafa Jabari, Davut Izci: Conceptualization, Methodology, Software, Visualization, Investigation, Writing-Original draft preparation. Serdar Ekinci, Lukas Prokop: Data curation, Validation, Supervision, Resources, Writing - Review & Editing. Mohit Bajaj, Vojtech Blazek: Project administration, Supervision, Resources, Writing - Review & Editing.

Declarations

Competing interests

The authors declare no competing interests.

Additional information

Correspondence and requests for materials should be addressed to M.B.

Reprints and permissions information is available at www.nature.com/reprints.

Publisher's note Springer Nature remains neutral with regard to jurisdictional claims in published maps and institutional affiliations.

Open Access This article is licensed under a Creative Commons Attribution-NonCommercial-NoDerivatives 4.0 International License, which permits any non-commercial use, sharing, distribution and reproduction in any medium or format, as long as you give appropriate credit to the original author(s) and the source, provide a link to the Creative Commons licence, and indicate if you modified the licensed material. You do not have permission under this licence to share adapted material derived from this article or parts of it. The images or other third party material in this article are included in the article's Creative Commons licence, unless indicated otherwise in a credit line to the material. If material is not included in the article's Creative Commons licence and your intended use is not permitted by statutory regulation or exceeds the permitted use, you will need to obtain permission directly from the copyright holder. To view a copy of this licence, visit http://creativecommons.org/licenses/by-nc-nd/4.0/.

© The Author(s) 2024